

RESEARCH ARTICLE

Differential expression of interferon-lambda receptor 1 splice variants determines the magnitude of the antiviral response induced by interferon-lambda 3 in human immune cells

Deanna M. Santer^{1*}, Gillian E. S. Minty¹, Dominic P. Golec², Julia Lu¹, Julia May¹, Afshin Namdar^{1,3,4}, Juhi Shah¹, Shokrollah Elahi^{1,3,4}, David Proud⁵, Michael Joyce¹, D. Lorne Tyrrell¹, Michael Houghton^{1*}

1 Li Ka Shing Institute of Virology and Department of Medical Microbiology and Immunology, University of Alberta, Edmonton, Alberta, Canada, **2** Alberta Diabetes Institute, University of Alberta, Edmonton, Alberta, Canada, **3** School of Dentistry, University of Alberta, Edmonton, Alberta, Canada, **4** Department of Oncology, University of Alberta, Edmonton, Alberta, Canada, **5** Department of Physiology and Pharmacology and Snyder Institute for Chronic Diseases, University of Calgary, Calgary, Alberta, Canada

* santer@ualberta.ca (DMS); mhoughto@ualberta.ca (MH)



OPEN ACCESS

Citation: Santer DM, Minty GES, Golec DP, Lu J, May J, Namdar A, et al. (2020) Differential expression of interferon-lambda receptor 1 splice variants determines the magnitude of the antiviral response induced by interferon-lambda 3 in human immune cells. *PLoS Pathog* 16(4): e1008515. <https://doi.org/10.1371/journal.ppat.1008515>

Editor: Jacob S. Yount, The Ohio State University, UNITED STATES

Received: December 3, 2019

Accepted: April 3, 2020

Published: April 30, 2020

Copyright: © 2020 Santer et al. This is an open access article distributed under the terms of the [Creative Commons Attribution License](https://creativecommons.org/licenses/by/4.0/), which permits unrestricted use, distribution, and reproduction in any medium, provided the original author and source are credited.

Data Availability Statement: All relevant data are within the manuscript and its Supporting Information files.

Funding: This work was supported by the Canada Excellence Research Chair Program (<https://www.cerc.gc.ca/home-accueil-eng.aspx>) (MH), and Alberta Innovates (<https://albertainnovates.ca/>) and Canada Institutes of Health Research (<http://www.cihr-irsc.gc.ca/e/193.html>) postdoctoral fellowships (DMS), and Canadian Institutes of

Abstract

Type III interferons (IFN-lambdas(λ)) are important cytokines that inhibit viruses and modulate immune responses by acting through a unique IFN- λ R1/IL-10RB heterodimeric receptor. Until now, the primary antiviral function of IFN- λ s has been proposed to be at anatomical barrier sites. Here, we examine the regulation of IFN- λ R1 expression and measure the downstream effects of IFN- λ 3 stimulation in primary human blood immune cells, compared with lung or liver epithelial cells. IFN- λ 3 directly bound and upregulated IFN-stimulated gene (ISG) expression in freshly purified human B cells and CD8⁺ T cells, but not monocytes, neutrophils, natural killer cells, and CD4⁺ T cells. Despite similar *IFNLR1* transcript levels in B cells and lung epithelial cells, lung epithelial cells bound more IFN- λ 3, which resulted in a 50-fold greater ISG induction when compared to B cells. The reduced response of B cells could be explained by higher expression of the soluble variant of IFN- λ R1 (sIFN- λ R1), which significantly reduced ISG induction when added with IFN- λ 3 to peripheral blood mononuclear cells or liver epithelial cells. T-cell receptor stimulation potently, and specifically, upregulated membrane-bound *IFNLR1* expression in CD4⁺ T cells, leading to greater antiviral gene induction, and inhibition of human immunodeficiency virus type 1 infection. Collectively, our data demonstrate IFN- λ 3 directly interacts with the human adaptive immune system, unlike what has been previously shown in published mouse models, and that type III IFNs could be potentially utilized to suppress both mucosal and blood-borne viral infections.

Health Research grants (360929, 353953) (SE). The funders had no role in study design, data collection and analysis, decision to publish, or preparation of the manuscript.

Competing interests: The authors have declared that no competing interests exist.

Author summary

Type III IFNs (IFN- λ s) are antiviral cytokines that are thought to act on specific subsets of cells, especially to protect mucosal barriers. Here, we demonstrate that IFN- λ 3 differentially binds multiple human immune cell subsets, indicating the specific receptor subunit, IFN- λ R1, is more broadly expressed in the human immune system, compared to published mouse models. IFN- λ R1 expression increased after cellular activation, and antiviral responses were inhibited by a soluble version of the receptor. The direct interaction of IFN- λ s with human immune cells, and specific regulation of IFN- λ R1 expression, has broad mechanistic implications in the modulation of inflammatory or anti-cancer immune responses, and future antiviral therapies.

Introduction

Type I and III interferons (IFNs) are induced in response to a variety of pathogens, and are responsible for the induction of a variety of ISGs that are essential for antiviral immune responses. While the type I IFN family was discovered in 1957 [1], the type III IFN family was discovered in 2003 [2–4]. There are four type III IFN (IFN- λ) family members: IFN- λ 1 (IL-29), IFN- λ 2 (IL-28A), IFN- λ 3 (IL-28B) and IFN- λ 4 [2, 3, 5, 6]. The majority of type III IFN studies have focused on the importance of type III IFNs in the defense against a number of viruses, especially at anatomical barriers [7–15]. In addition, multiple genome wide association studies have demonstrated the importance of the *IFNL3/4* locus in both IFN- α treatment response and the natural clearance of the hepatitis C virus (HCV) [16–18]. Type III IFNs can also significantly dampen inflammation in mouse models of allergic asthma, colitis, and autoimmune arthritis [19–22]. Differences in biological activities between type I and type III IFNs likely relate to differences in cell-type specific receptor expression, and potency and kinetics of signaling, where IFN- λ s induce a slower, prolonged, lower magnitude response [23, 24]. It has been proposed that IFN- λ s could act as an initial defense to inhibit virus replication without causing inflammation, before type I IFNs are induced [25, 26].

All type III IFN family members signal through a unique heterodimeric receptor comprised of IFN- λ R1 (IL-28RA) and IL-10RB [2, 3, 27]. Similar to type I IFNs, type III IFNs induce ISGs by activating JAK1 and TYK2, which associate with IFN- λ R1 and IL-10RB, respectively, leading to the phosphorylation of STAT1/STAT2 and ISG induction [28–30]. Unlike the type I IFN receptor (IFNAR1/2) and IL-10RB, which are ubiquitously expressed on virtually all nucleated cells, IFN- λ R1 expression is more restricted. *IFNL1* transcripts and/or IFN- λ responsiveness has been observed in epithelial cells of the lung, liver, and gut [28, 31–33], endothelial cells of the blood brain barrier [11] and trophoblasts within a placenta [34]. Multiple splice variants of *IFNL1* have been described in human cells [3, 4, 35], but the majority of work has focused on the full length, membrane form (*mIFNL1*), with little data reported on the biological effects of the soluble form (*sIFNL1*) in which the transmembrane domain is deleted. Within the immune system, human plasmacytoid dendritic cells (pDCs) strongly respond to IFN- λ s, but little or no IFN- λ R1 transcript has been found in monocytes, natural killer cells, or T cells [7, 35–44]. Transcripts for *IFNL1* are detectable in human, but not mouse B cells [20, 45], but the human B cell response to IFN- λ s has not been consistently demonstrated [7, 35, 44, 45]. In mouse models of infection or autoimmunity, neutrophils are the major immune cell type that express high levels of *Ifnlr1* transcripts and can potently respond to IFN- λ s [19, 20, 25, 46], but more work is needed to determine if IFN- λ s directly stimulate ISGs in human neutrophils.

Previously, we demonstrated that IFN- λ 3 inhibited human B cell antibody production and decreased the Th2 response to an H1N1 influenza vaccine antigen [47], but it is not clear which human immune cells directly respond to IFN- λ 3. Here, we investigate and quantify expression of IFN- λ R on human immune cells and correlate these findings with ISGs induced by IFN- λ 3. We demonstrate that human adaptive immune cells express both IFN- λ R1 variants (mIFN- λ R1, sIFN- λ R1), where sIFN- λ R1 inhibits ISG induction by IFN- λ 3. In addition, we show mIFN- λ R1 expression varies between cell subsets and can be upregulated by activation of immune cell receptors including the T-cell receptor (TCR), B-cell receptor (BCR) and Toll-like receptors (TLR). In purified activated CD4⁺ T cells, IFN- λ 3 pretreatment leads to antiviral ISG induction and a significant decrease in HIV-1 infection. Taken together, these results show that unlike in mice, IFN- λ 3 directly regulates the human adaptive immune system and may be exploited in the future to promote type 1 and antiviral responses and dampen type 2 immune responses.

Results

IFN- λ R1 is differentially expressed among peripheral human immune cell subsets

Recent type III IFN studies have focused on their antiviral or protective effects in epithelial cells at barrier sites, but consensus is lacking regarding which human immune cells express the IFN- λ R. We first quantified transcript levels of both subunits of IFN- λ R (*IFNLR1* and *IL10RB*) in highly pure immune cell subsets from blood of healthy individuals, primary human hepatocytes, and normal human bronchial epithelial cells (NHBE). We found, as expected, ubiquitous *IL10RB* expression, with the highest levels found in monocytes and neutrophils (Fig 1A). The highest expression of *IFNLR1* transcripts were found in epithelial cell types and B cells, while CD4⁺ and CD8⁺ T cells expressed less *IFNLR1* mRNA, and monocytes, natural killer cells, and neutrophils had little or barely detectable expression levels of *IFNLR1* transcript (Fig 1A). CD8⁺ T cells had significantly greater expression of *IFNLR1* compared to CD4⁺ T cells ($P = 0.0021$). This is the first report of differential expression of *IFNLR1* in human CD4⁺ versus CD8⁺ T cells. Our results contrast those in mice where *Ifnlr1* transcript expression is highest in neutrophils and little or no expression can be detected in all other immune cell types [20, 25].

IFN- λ 3 binds to both epithelial cells and specific immune cell subsets

To date, studies on IFN- λ R1 biology have been limited due to a lack of sensitive reagents to measure receptor protein expression. We recently developed a flow cytometry binding assay [48], which measures IFN- λ 3 binding to the cell surface as a surrogate of IFN- λ R1 expression. We quantified the binding of 6 His-tagged IFN- λ 3 to immune cell subsets within peripheral blood, as well as primary liver and lung epithelial cells. Our flow cytometry gating strategy for PBMCs and neutrophils is shown in S1 and S2 Figs. Multiple immune cell subsets bound IFN- λ 3 in a dose-dependent manner, and the maximum binding percentage was dependent on the cell type (Fig 1B). Almost 100% of hepatocytes and NHBE cells bound IFN- λ 3 at the highest dose tested (Fig 1B), and the amount of IFN- λ 3 bound (median PE value) was 4.4–11.7 fold greater than what bound to immune cell subsets (S3A Fig). The binding results were very reproducible within a single donor; the percentage of monocytes or B cells that bound IFN- λ 3 did not vary substantially when the same assay was repeated at least six months later (S3B Fig). An unrelated 6 His-tagged protein (OBCAM) did not significantly bind any of the cell types examined (Fig 1C and S3C Fig). IFN- λ 3 also did not significantly bind Huh7 *IFNLR1* knock-out cells, which were previously shown to be unresponsive to IFN- λ 3 stimulation [49] (S3D

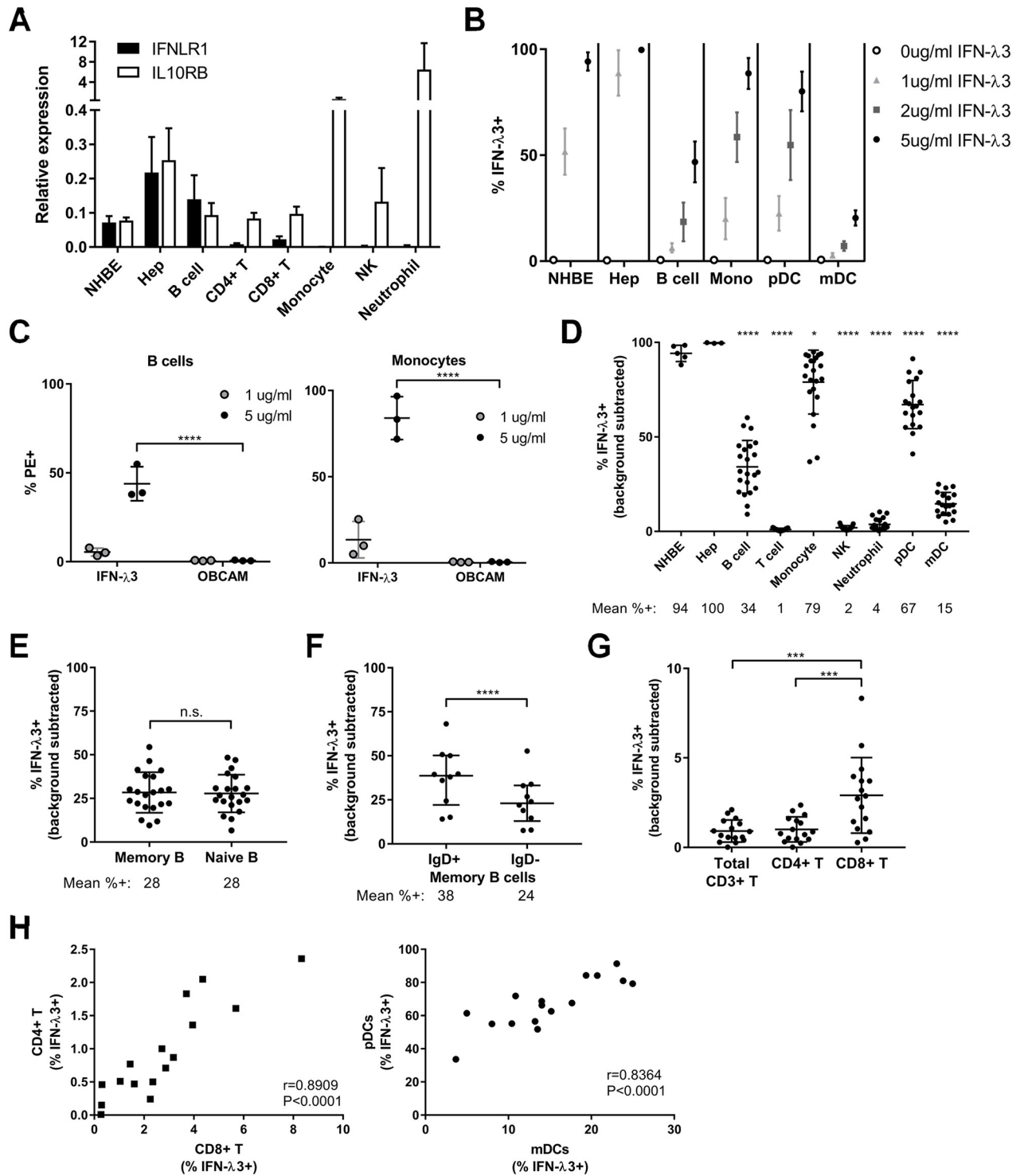


Fig 1. Differential IFN-λR expression and IFN-λ3 binding among primary human immune and epithelial cells. A) Normalized expression values for each subunit of the IFN-λR as determined by RT-qPCR for normal human bronchial epithelial cells (NHBE), primary hepatocytes (hep) or immune cells purified from healthy human donor blood. Graph shows mean + SEM for 3–7 different donors for each population. Results were normalized to the geomean of HPRT1 and RPL13A reference genes. B–H) IFN-λ3 binding was quantified via flow cytometry as described in the Materials and Methods. B) Dose curves of adding 1, 2 or 5 μg/ml IFN-λ3 to epithelial cells or total human PBMCs. 0 μg/ml IFN-λ3 refers to adding the secondary antibody alone. Graph shows mean +/- SD for 3–7 different donors. C) Binding percentages as detected by flow cytometry for IFN-λ3 or a similarly His-tagged control protein (OBCAM) where means +/- SD are shown. D–H) Quantified IFN-λ3 (5 μg/ml) binding percentages to each cell type where each dot represents a different healthy individual and background binding of the secondary antibody alone was subtracted. In D),

statistical significance results were identical when comparing either NHBE or hep to all other immune cell subsets. All comparisons are shown in [S1 Table](#). H) Pearson correlation coefficients (r) calculated when comparing IFN- λ 3 binding to different immune cell subsets. All comparisons are shown in [S2 Table](#). *, $P < 0.05$, ***, $P < 0.001$, ****, $P < 0.0001$, two-way (C) or one-way (D, G) ANOVA with Tukey's multiple comparisons test, paired t-test (E-F).

<https://doi.org/10.1371/journal.ppat.1008515.g001>

[Fig](#)). Consistent with previous reports that pDCs respond to IFN- λ stimulation [[41](#), [43](#), [44](#)], IFN- λ 3 bound to pDCs at high levels ([Fig 1B and 1D](#)). B cells, monocytes, pDCs, and mDCs all bound IFN- λ 3, whereas little IFN- λ 3 bound to total T cells, NK cells, and neutrophils ([Fig 1B and 1D](#)). IFN- λ 3 bound a significantly higher percentage of hepatocytes and NHBE cells compared with all immune cell subsets tested ([Fig 1D](#), [S1 Table](#)). While there was no difference in IFN- λ 3 binding between memory and naïve B cells, we observed significantly higher binding of IFN- λ 3 to IgD⁺ versus IgD⁻ memory B cells ([Fig 1E and 1F](#)). CD8⁺ T cells also bound significantly more IFN- λ 3 than CD4⁺ T cells ([Fig 1G](#)), consistent with the greater *IFNL1* transcripts measured in CD8⁺ T cells ([Fig 1A](#)). Next, we examined whether the percentage of IFN- λ 3 binding correlated between immune cell subsets within each donor. We found there was significant correlation between cell types, especially within the same immune cell lineage. For example, the levels of IFN- λ 3 binding to CD4⁺ T cells positively correlated with the percentage bound to CD8⁺ T cells, and similarly, the binding of IFN- λ 3 to pDCs positively correlated with the binding to mDCs ([Fig 1H](#)). Correlation results between immune cell subsets are shown in [S2 Table](#) and [S4 Fig](#). The binding of IFN- λ 3 to the cell surface matched the relative expression of *IFNL1* transcripts quantified in [Fig 1A](#) for most immune cell subsets. The exception was monocytes where little *IFNL1* transcript was detectable, but IFN- λ 3 binding was observed. Interestingly, despite comparable *IFNL1* mRNA levels in B cells and NHBE cells ([Fig 1A](#)), significantly higher amounts of IFN- λ 3 bound to NHBE cells than B cells ($P < 0.0001$) ([Fig 1B and 1D](#) and [S3A Fig](#)). Collectively, these results show that primary epithelial cells and specific human immune cell subsets bind IFN- λ 3, but epithelial cells bind IFN- λ 3 at a much higher level.

IFN- λ 3 binding leads to ISG induction in both epithelial cells and specific immune cell subsets

Previous studies that examined IFN- λ R expression and IFN- λ stimulation of human immune cells had conflicting results [[35](#), [39](#), [44](#), [45](#), [50](#)]. Since we observed dramatic differences in IFN- λ 3 binding by immune cell subsets, we next determined whether the amount of IFN- λ 3 bound by each subset mirrored the relative induction of ISGs upon IFN- λ 3 stimulation. We compared IFN- λ 3 responses in highly pure B cells, monocytes, CD4⁺ T cells, CD8⁺ T cells, or neutrophils freshly isolated from peripheral blood of healthy donors. Representative results of the purity of our isolated cell subsets are shown in [S2](#) and [S5 Figs](#). For all cell types except neutrophils, we added recombinant IFN- λ 3 overnight to induce ISG expression. Neutrophils were treated with IFN- λ 3 for 5 hours since the majority of neutrophils die during overnight culture *in vitro* [[51–53](#)]. Among immune cells, the greatest ISG response to IFN- λ 3 was seen in B cells, consistent with their expression of *IFNL1* and IFN- λ 3 binding potential ([Fig 2A](#)). Low levels of ISGs were induced by IFN- λ 3 in CD4⁺ T cells with the highest induction of *OAS1* (mean 2.9 fold upregulation in IFN- λ 3 treated versus unstimulated control), whereas all ISGs tested were induced by IFN- λ 3 in CD8⁺ T cells (mean 4.8 to 8.2 fold upregulation in IFN- λ 3 treated versus unstimulated control). Baseline expression of all 3 ISGs was not statistically different between B cells, CD4⁺ T cells and CD8⁺ T cells, therefore the higher response in B cells was not due to lower ISG expression prior to IFN- λ 3 stimulation ([S6A Fig](#)). In contrast, neutrophils had significantly greater baseline IFIT1 and ISG15 expression compared to B and T cells, in

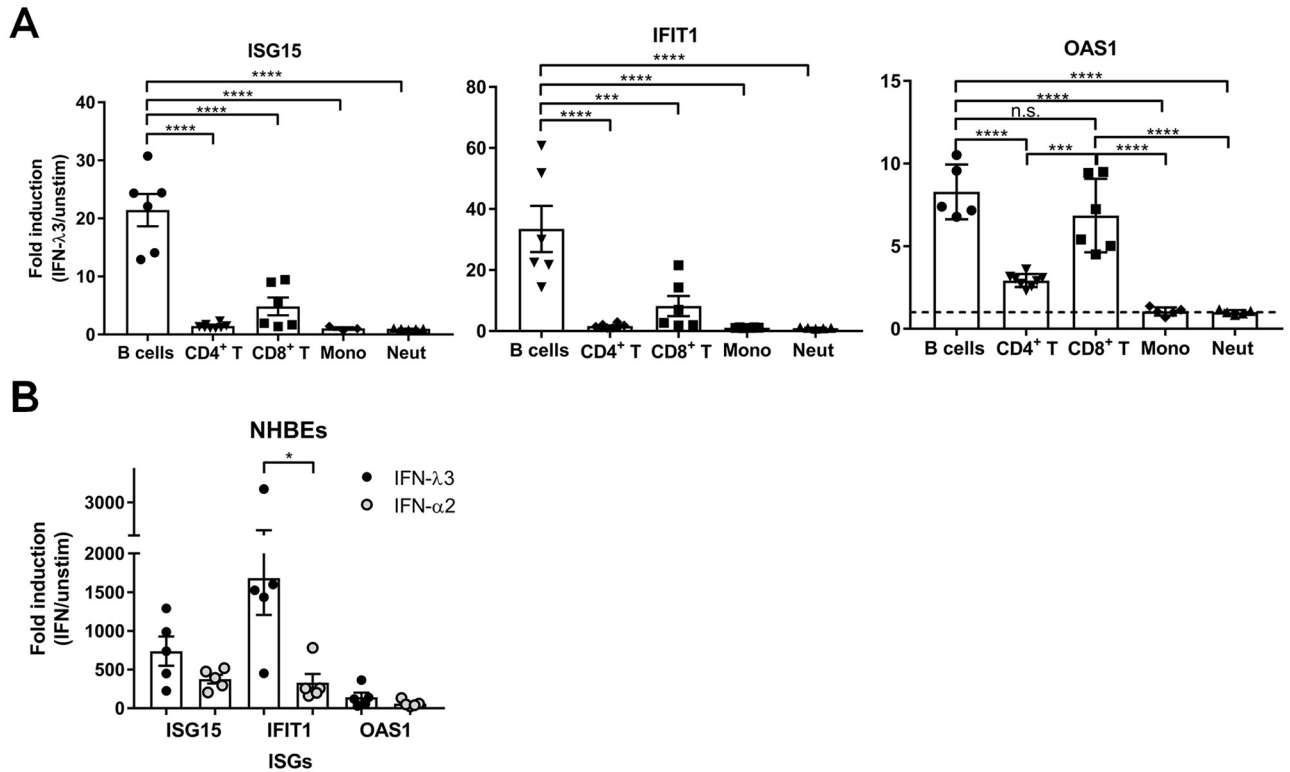


Fig 2. IFN-λ3 mediated ISG induction in primary human lung epithelial cells, B cells and T cells, but not monocytes or neutrophils. A-B) RT-qPCR quantification of ISG15, IFIT1, and OAS1 induced by IFN-λ3 (100 ng/ml) purified human immune cell subsets (A) or normal human bronchial epithelial cells (NHBEs) (B). All cell types were cultured with or without IFN-λ3 for 24 hrs, except neutrophils (5 hrs). Graphs show fold induction relative to unstimulated cells after normalization to the geomean of HPRT1 and RPL13A reference genes. Bars represent mean +/- SEM from 3–8 different donors. n.s., not significant, *, P<0.05. ***, P<0.001, ****, P<0.0001, one-way ANOVA, Tukey’s multiple comparisons test (A), paired t-test (B).

<https://doi.org/10.1371/journal.ppat.1008515.g002>

agreement with published microarray and single cell RNA sequencing data [54, 55] (S6A Fig). OAS1 expression was not significantly different between B cells and neutrophils or monocytes. Overall, our results indicate both B and T cells can directly respond to IFN-λ3, but with different magnitudes. Both monocytes and neutrophils failed to upregulate ISGs in response to IFN-λ3 (Fig 2A), demonstrating that the IFN-λ3 we detected bound to monocytes in our binding assay does not induce ISG induction, at least under the conditions tested. All immune cell types tested responded to our positive control IFN-α2 (S6B Fig).

Since we observed greater IFN-λ3 binding to NHBE cells compared to B cells despite higher relative *IFNL1* transcript expression in B cells, we next quantified ISG induction by IFN-λ3 in NHBE cells. When NHBE cells were treated with IFN-λ3 overnight, high levels of ISGs were induced (Fig 2B). At this time point, ISG induction by IFN-λ3 was significantly higher than the levels we observed with IFN-α2 treatment for most genes tested (Fig 2B). There was up to 50-fold higher ISG induction by IFN-λ3 in NHBE cells compared to B cells (Fig 2A and 2B). We confirmed NHBE and B cells had comparable baseline ISG expression (S6A Fig). This result matched our cell surface IFN-λ3 binding quantification, which was ~5 fold higher in NHBE cells compared to B cells (S3A Fig). We then recapitulated this phenomenon in cell lines. The DG75 B cell line expressed on average 2.8 fold greater *IFNL1* mRNA than the BEAS-2B bronchial lung epithelial cell line, although greater *IL10RB* expression was found in BEAS-2B cells (Fig 3A). Analogous to our results in primary cells, BEAS-2B lung epithelial

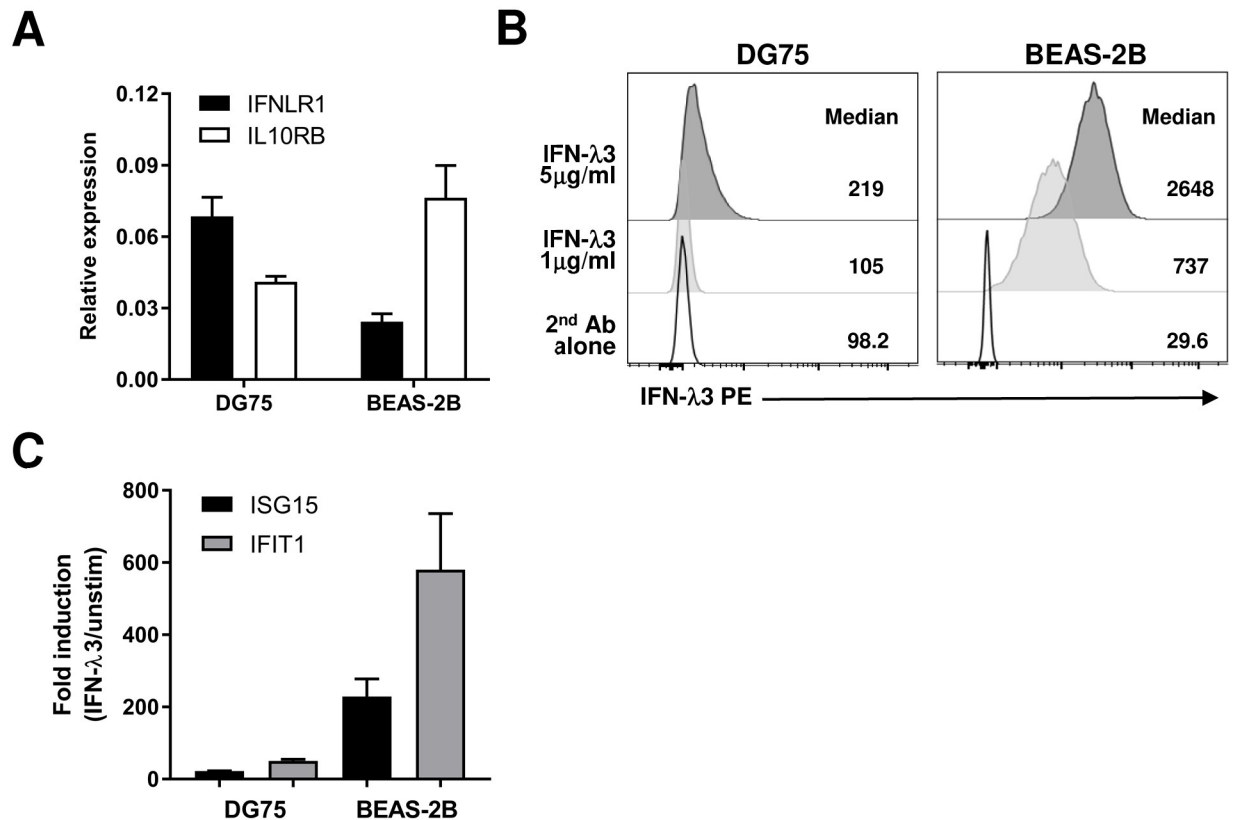


Fig 3. Greater IFN-λ3 cell surface binding and ISG induction in BEAS-2B bronchial epithelial cell line compared to DG75 B cell line mimics results seen in primary cells. A) Normalized expression values for each subunit of the IFN-λR as determined by RT-qPCR for DG75 or BEAS-2B cell lines. Results were normalized to the geometric mean of *HPRT1* and *RPL13A* reference genes. B) IFN-λ3 flow cytometry binding assay results for 0, 1, or 5 μg/ml His-tagged IFN-λ3 added to DG75 or BEAS-2B cells. C) RT-qPCR quantification of *ISG15* and *IFIT1* mRNA in DG75 or BEAS-2B cells induced by IFN-λ3 (100 ng/ml) as compared to unstimulated cells after 24 hrs incubation. Bar graphs (A, C) show means + SEM from 2 independent experiments and flow cytometry histograms (B) are representative of 2 independent binding assays.

<https://doi.org/10.1371/journal.ppat.1008515.g003>

cells bound dramatically more IFN-λ3 at the cell surface compared to DG75 B cells with 7–12 fold higher median fluorescent intensities detected (Fig 3B). This increased IFN-λ3 cell surface binding translated to 10–11 fold greater ISG induction in BEAS-2B cells compared to DG75 B cells in response to overnight IFN-λ3 treatment (Fig 3C). Our results demonstrated that our IFN-λ3 binding assay is a useful tool to predict IFN-λ3 responsiveness. While previous studies have solely quantified *IFNLR1* mRNA and because a sensitive antibody is not commercially available, one must be cautious that total *IFNLR1* transcript levels do not necessarily correlate with IFN-λ3 induced ISGs.

Soluble IFN-λR1 directly binds cells to increase IFN-λ3 binding to the surface but inhibits ISG induction

To further examine the discrepancy between high and similar levels of *IFNLR1* transcript seen in both B cells and lung epithelial cells, but low B cell ISG expression in response to IFN-λ3, we determined if sIFN-λR1 plays a role in controlling ISG responses. This variant lacks a transmembrane domain and was detectable in cell line supernatants when overexpressed [35]. Little is known about the regulatory role of sIFN-λR1 in IFN-λ biology except that pre-incubating 100–1000 fold excess sIFN-λR1 with IFN-λ1 inhibited MHC class I upregulation on the

HepG2 hepatocyte cell line [35]. We used our previously designed RT-qPCR assay to specifically quantify either the full length membrane form (*mIFNLR1*) or *sIFNLR1* [48]. Using this assay, we found all immune cells tested had higher levels of *sIFNLR1* relative to *mIFNLR1*, when compared to epithelial cells. The membrane/soluble receptor transcript ratio was 0.6–2 in immune cells, whereas in lung or liver epithelial cells it was 9.4–17.6 (Fig 4A). B cells had similar *mIFNLR1* mRNA expression, but higher *sIFNLR1* levels compared to epithelial cells. CD8⁺ T cells expressed the next highest transcript level of *mIFNLR1* at 3-fold higher levels than CD4⁺ T cells. Monocytes and NK cells expressed very little or no *IFNLR1* mRNA of either variant. Neutrophils were the only cell type tested where there was higher *sIFNLR1* than *mIFNLR1* expression (Fig 4A). In agreement with our data with primary T and B cells, we had previously found Jurkat T cell and Raji B cell lines also had low membrane/soluble *IFNLR1* ratios of ~2–3 [48]. We extended our cell line results to demonstrate that the lung BEAS-2B and A549 epithelial cell lines had a much higher membrane/soluble *IFNLR1* transcript ratio of 14.9 and 6.7 respectively, while DG75 B cells had a lower ratio of 4.0 (Fig 4A). Our results indicate that the varied expression of *sIFNLR1* may relate to extent of the ISG response induced by IFN- λ 3.

To examine if sIFN- λ R1 regulates IFN- λ 3-mediated ISG responses, we added recombinant sIFN- λ R1 protein alongside IFN- λ 3 to PBMCs and then quantified ISG induction. The addition of sIFN- λ R1 dramatically inhibited ISG induction by an average of 54–78% (Fig 4B). This inhibition of IFN- λ 3 activity was not unique to immune cells because sIFN- λ R1 similarly inhibited IFN- λ 3-mediated ISG induction in the Huh7.5 hepatocyte cell line (Fig 4C). Since soluble cytokine receptors can act to prevent cytokine binding to the cell surface, or can act directly at the cell surface interacting with co-receptors [56], we first determined if sIFN- λ R1 could bind the cell surface in the absence or presence of IFN- λ 3 cytokine. Surprisingly, sIFN- λ R1 bound both primary immune cells within PBMCs (Fig 4D), and epithelial cell lines (Fig 4E) in the absence of IFN- λ 3. This binding was not due to the Fc tag on recombinant IFN- λ R1, since excess human IgG was added first to block Fc receptors, and recombinant IL-10RB with the same Fc tag did not bind any cell type tested (Fig 4D and 4E). Among peripheral immune cells, more primary monocytes bound sIFN- λ R1 than any other cell type, but A549 and Huh7.5 epithelial cell lines required ~100-fold less sIFN- λ R1 protein to bind similar levels of sIFN- λ R1 as monocytes (0.01 μ g/ml epithelial cells versus 1 μ g/ml for monocytes) (Fig 4D and 4E). Due to the secondary anti-Fc antibody binding to surface IgG on primary B cells, we did not include B cell results in our analysis. We visualized sIFN- λ R1 binding to the cell surface of four cell lines using imaging flow cytometry. We observed a distinct cell surface staining pattern with higher levels of sIFN- λ R1 on the surface of A549 and Huh7.5 epithelial cell lines compared to THP-1 monocytes and Jurkat T cells (median 8–10 fold greater despite 2-fold less sIFN- λ R1 added) (Fig 4F). Addition of IFN- λ 3 protein to cells simultaneously with sIFN- λ R1 did not increase sIFN- λ R1 binding to Huh7.5 cells (S7A Fig). Taken together, we have shown for the first time that sIFN- λ R1 can bind multiple cell types without requiring previous interaction with IFN- λ cytokine.

After observing striking differences in binding of sIFN- λ R1 to various cell types, we next utilized our IFN- λ 3 binding assay to determine if sIFN- λ R1 binding to the cell surface affects IFN- λ 3 binding. The addition of recombinant sIFN- λ R1 with IFN- λ 3 to PBMCs led to 5–15 fold greater binding of IFN- λ 3 to the surface of B cells, monocytes, and T cells compared to IFN- λ 3 alone at the highest dose tested (Fig 4G and 4H). Addition of sIFN- λ R1 also increased binding of IFN- λ 3 to Huh7.5 cells in a dose-dependent manner (S7B Fig). Allowing sIFN- λ R1 to bind first to cells before adding IFN- λ 3, or adding them simultaneously, resulted in the equivalent increased binding of IFN- λ 3 compared to adding cytokine alone (S7C Fig). Recombinant IL-10RB or denatured sIFN- λ R1 at the same concentrations did not increase IFN- λ 3

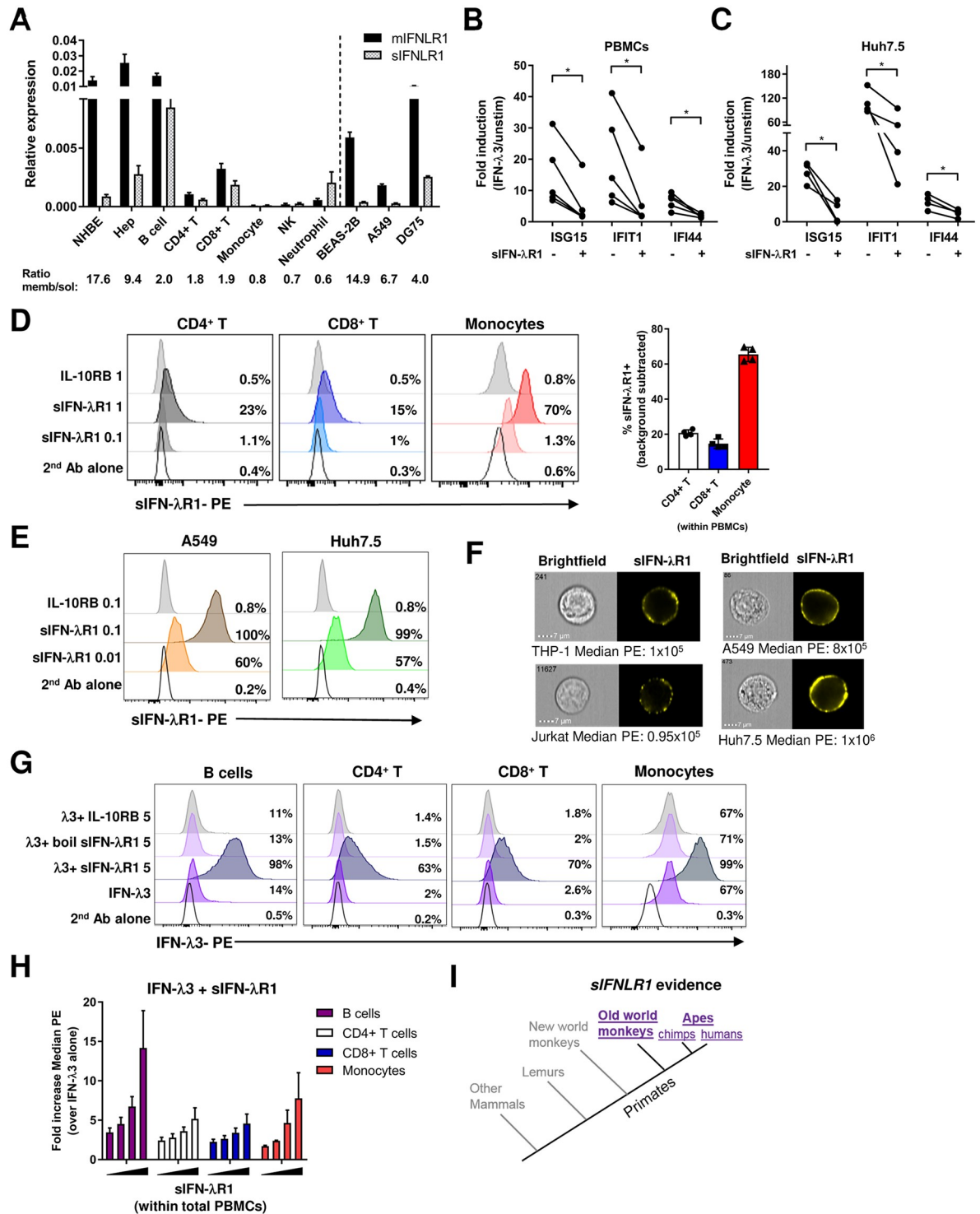


Fig 4. Soluble IFN-λR1 found in primates binds to the cell surface to increase binding of IFN-λ3 but inhibits ISG induction. A) Normalized expression values for each variant of *IFNLR1* (membrane, full length (*mIFNLR1*), or small, soluble (*sIFNLR1*)) as determined by RT-qPCR for normal human bronchial epithelial cells (NHBE), hepatocytes (hep) or immune cells purified from healthy human donor blood, or cell lines (BEAS-2B or A549 lung epithelial or DG75 B cell). Means + SEM are shown from 3–6 different donors (primary cells) or 2–3 independent experiments (cell lines). Results were normalized to the geomean of *HPRT1* and *RPL13A* reference genes. B–C) Fold induction of 3 ISGs (ISG15, IFIT1, IFI44) by IFN-λ3 (10 ng/ml) treatment of total PBMCs (B) or Huh7.5 hepatocytes (C) relative to unstimulated cells with or without simultaneous addition of recombinant sIFN-λR1 (100 ng/ml (PBMC), 1000 ng/ml (Huh7.5)). Each dot represents a different individual or experiment. D–E) Quantification of binding of recombinant sIFN-λR1 or control IL-10RB to individual

cell subsets within total PBMCs (D), or to A549 or Huh7.5 cell lines (E). Binding was detected by anti-Fc PE antibody. Histograms are representative of results from 4 different PBMC donors (bar graph right panel D), or from 2–3 independent experiments (E). F) Imaging flow cytometry visualization of binding of sIFN- λ R1 (500 ng/ml (A549, Huh7.5), 1 μ g/ml (THP-1, Jurkat)) to 4 cell lines. The median PE intensity is shown below each representative image from 6,000–12,000 total cells acquired from 2–3 independent experiments. G–H) IFN- λ 3 binding to cell subsets within PBMCs where IFN- λ 3 (2 μ g/ml) was added with or without sIFN- λ R1 (0.5–5 μ g/ml +/- boiling) or IL-10RB (5 μ g/ml). Percent IFN- λ 3 bound and fold increase in median PE fluorescence are representative from 2–4 donors (G) or plotted as means + SD from 2–4 different donors (H). I) The presence of a soluble *IFNL1* variant within primates and lower mammals. Gray indicates no annotation and no transcript detectable in deposited RNA sequencing data, and purple indicates both annotation and detection of RNA transcript in multiple cell types from deposited RNA sequencing data. *, $P < 0.05$, paired t-tests (B–C).

<https://doi.org/10.1371/journal.ppat.1008515.g004>

binding to any cell type tested (Fig 4G). These results could help explain why B cells are less responsive to IFN- λ 3 compared to lung epithelial cells despite similar *IFNL1* transcript expression. Taken together, our data shows sIFN- λ R1 increased IFN- λ 3 binding to the cell surface, potentially through interactions with IL-10RB, the second subunit of the IFN- λ R. This binding would prevent ISG induction though, because the cytoplasmic tail, not present in sIFN- λ R1, is required for downstream signaling [29]. Lower levels of sIFN- λ R1 at epithelial barriers could explain why those cell types are especially responsive to type III IFNs.

Soluble *IFNL1* evolved late in evolution with detectable transcripts in specific primates

Our data describing which human immune cell express total *IFNL1* transcripts contrast published mouse cell *Ifnlr1* expression, but previous studies had only measured *sIFNL1* transcripts in human cells [3, 4, 35]. We next investigated whether other primates and lower mammals such as mice also encoded for a soluble form of *IFNL1*. We found that the *sIFNL1* transcript variant missing the transmembrane domain (exon 6) is only annotated in primates, specifically most old world monkeys and all apes, but not in new world monkeys, lemurs, tarsiers and lower mammals with the exception of the guinea pig (Fig 4I and S3 Table). To examine if annotations were missing for *sIFNL1* and to find experimental evidence of *sIFNL1* expression, we BLAST searched the NCBI Sequence Read Archive (SRA) using a 120 nucleotide sequence spanning the end of exon 5 and beginning of exon 7 for each species of interest. We found detectable *sIFNL1* transcripts in experiments with cells from apes and certain old world monkeys in multiple tissues including epithelial cells and immune cells, but *sIFNL1* transcripts could not be detected in any experimental data deposited for lower mammals, including the potential variant annotated in guinea pigs. A full summary of species studied and example data accession numbers are listed in S3 Table. These results are consistent with the late evolution of the soluble variant of IFN- λ R1 in mammals, with only the closest relatives of humans having experimental evidence for the expression of *sIFNL1*.

Stimulation of B cells and neutrophils upregulates IFN- λ R1 expression

The differential expression of IFN- λ R1 on the surface of different human immune cell subsets implied that IFN- λ R1 expression can be regulated. We therefore examined whether IFN- λ R1 expression could be altered by adding various stimuli to B cells or neutrophils. B cells were chosen because they represent cells that express high levels of *IFNL1*, while neutrophils have little *IFNL1* transcript expression. Previous work had shown that IFN- α significantly upregulated *IFNL1* mRNA in human hepatocytes [9], so we tested whether this regulation also occurred in immune cells. Stimulation of PBMCs for 3 days with anti-BCR (IgM/IgG/IgA) and anti-CD40 or the TLR7/8 ligand R848, but not the cytokines IFN- γ or IFN- α 2, increased IFN- λ 3 binding to total B cells (Fig 5A). Surprisingly, IFN- α 2 treatment significantly decreased the percent of total B cells binding IFN- λ 3 by 62% on average (Fig 5A). We performed a

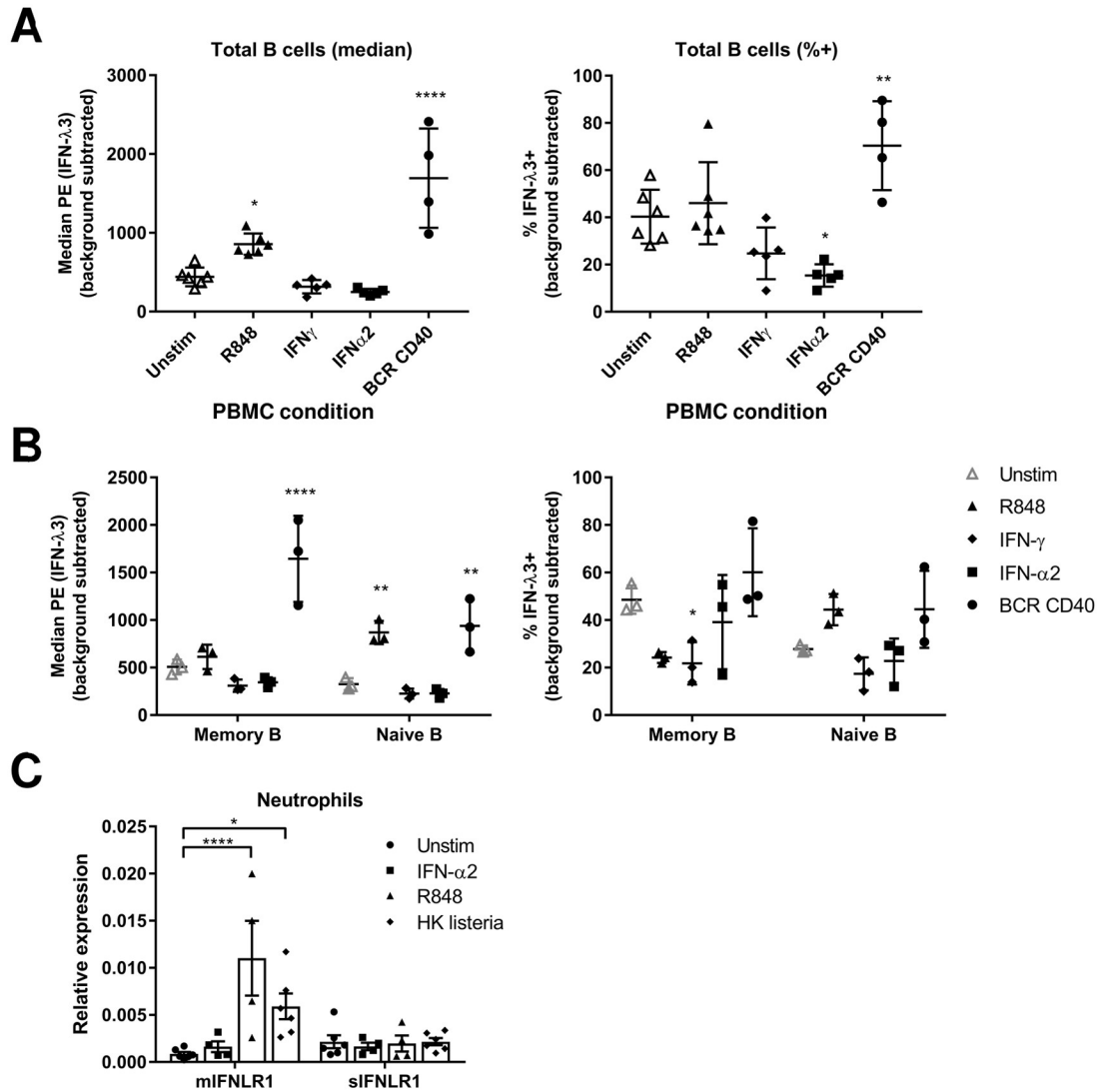


Fig 5. BCR or TLR activation upregulate IFN-λ3 binding and IFN-λR1 expression. A-C) IFN-λ3 (5 μg/ml) binding to LIVE/DEAD⁻ CD20⁺ B cells (A-B, memory (CD27⁺), naïve (CD27⁻)) or CD3⁺ CD4⁺ or CD8⁺ T cells (C) within total PBMCs that had been cultured for 3 days either unstimulated (unstim), or with the following stimuli: R848 (1 μg/ml), IFN-γ (10 ng/ml), IFN-α2 (1000 IU/ml) or anti-IgM/IgG/IgA (BCR, 10 μg/ml) and anti-CD40 (5 μg/ml). The percent IFN-λ3⁺ or median PE fluorescence is shown after background subtraction of secondary antibody alone with means ± SD. C) RT-qPCR quantification of *sIFNLR1* and *mIFNLR1* transcripts in purified neutrophils that were left unstimulated (unstim) or stimulated with IFN-α2 (1000 IU/ml), R848 (1 μg/ml) or heat killed listeria (HK listeria) supernatant (1:100) for 5 hrs. *, P<0.05, **, P<0.01, ****, P<0.0001, one-way ANOVA (A) or two-way ANOVA (B-C), Dunnett's multiple comparisons test between each treatment and unstimulated. Only significant comparisons are noted and each symbol represents a different individual donor.

<https://doi.org/10.1371/journal.ppat.1008515.g005>

similar analysis to compare naïve and memory B cells within PBMCs. R848 treatment significantly upregulated IFN-λ3 binding fluorescence to naïve B cells, but not memory B cells, whereas IFN-γ addition specifically decreased IFN-λ3 binding to memory B cells (Fig 5B).

Similar to B cells, when purified human neutrophils were stimulated with R848 for 5 hours, the transcript for *mIFNLR1* was significantly upregulated (Fig 5C). The addition of heat killed listeria bacteria supernatant, which would stimulate multiple pattern recognition receptors, also significantly upregulated *mIFNLR1* transcript expression (Fig 5C). *sIFNLR1* transcript expression was not significantly altered in any neutrophil stimulation assay. Collectively, our

data demonstrate that receptor stimulation of B cells and neutrophils can upregulate surface expression of IFN- λ R1. Therefore, during an infection or inflammatory state, multiple immune cell types could have greater responsiveness to type III IFNs.

Stimulation of CD4⁺ T cells via the TCR upregulates IFN- λ R1 expression and IFN- λ 3 induced ISG expression

Given that BCR and TLR activation upregulated IFN- λ R1 expression on B cells and neutrophils, we hypothesized that the low *IFNLR1* expression observed in CD4⁺ T cells could also be modulated with appropriate T cell specific stimulation. In addition, we and others have shown IFN- λ s modulate Th2 cytokine production [6, 21, 57], therefore understanding if IFN- λ R1 expression changes upon stimulation has direct implications in elucidating mechanistically how Th2 responses are regulated. Only stimulating the TCR with anti-CD3/anti-CD28 antibodies significantly upregulated IFN- λ 3 binding to CD4⁺ T cells (Fig 6A). R848 has limited activation potential with human T cells in the absence of other signals [58], therefore R848 activating monocytes and B cells during the 3 day culture did not indirectly upregulate IFN- λ 3 binding to CD4⁺ T cells. We further investigated changes in IFN- λ R expression at the transcript level in sorted CD4⁺ T cells. We found total *IFNLR1*, but not *IL10RB*, mRNA was significantly increased by TCR stimulation (Fig 6B). Interestingly, only the signaling capable *mIFNLR1*, but not *sIFNLR1*, was upregulated by TCR stimulation (Fig 6C). The *mIFNLR1/sIFNLR1* ratio for CD4⁺ T cells had increased from an average of 2.5 at day 0 to 8.0 at day 3, bringing it closer to ratios we previously observed in epithelial cells. This is the first report of specific regulation of *mIFNLR1* expression by TCR stimulation. We next examined whether TCR upregulation of *IFNLR1* enhanced IFN- λ 3 responsiveness. Stimulation of PBMC cultures with anti-CD3/anti-CD28 for 3 days followed by IFN- λ 3 addition to sorted CD4⁺ T cells led to enhanced ISG induction for 2 of 3 ISGs tested (Fig 6D). Altogether, our data demonstrate TCR stimulation significantly increases mIFN- λ R1 expression on CD4⁺ T cells leading to greater ISG induction in response to IFN- λ 3.

IFN- λ 3 treatment inhibits HIV-1 infection of purified CD4⁺ T cells

To examine the consequence of increased IFN- λ R1 expression on CD4⁺ T cells, we determined if IFN- λ 3 could directly inhibit a viral infection of CD4⁺ T cells. We used HIV-1 infection of purified CD4⁺ T cell cultures to monitor whether pre-incubation of IFN- λ 3 before HIV-1 inoculation leads to decreased viral infection in the absence of any other immune cells. Optimal HIV-1 infection requires T cell activation [59, 60], therefore we purified total CD4⁺ T cells and activated them with PHA for 3 days. PHA activation upregulated *mIFNLR1* mRNA 2.4 fold on average, but did not upregulate *sIFNLR1* expression (Fig 7A). As expected, subsequent IFN- λ 3 treatment of PHA activated CD4⁺ T cells stimulated significant ISG expression compared to no cytokine treated controls (Fig 7B). Next, we tested whether IFN- λ 3 induced an antiviral state in PHA-stimulated CD4⁺ T cells. We added IFN- λ 3, or pegylated IFN- α 2 as our positive control, for 24 hours prior to HIV-1 infection. CD4⁺ T cells treated with either IFN- λ 3 or IFN- α 2 had significantly decreased HIV-1 p24 positive cells, indicating IFN- λ R or IFN- α R signaling inhibited HIV-1 infection (Fig 7C and 7D). These data indicate that type III IFNs can directly impact antiviral responses of peripheral blood CD4⁺ T cells to inhibit HIV-1 infection.

Discussion

The lack of a sensitive IFN- λ R1 antibody has limited our understanding of IFN- λ R1 biology in the context of human immune cells. Here, we have clearly identified the main cell types that

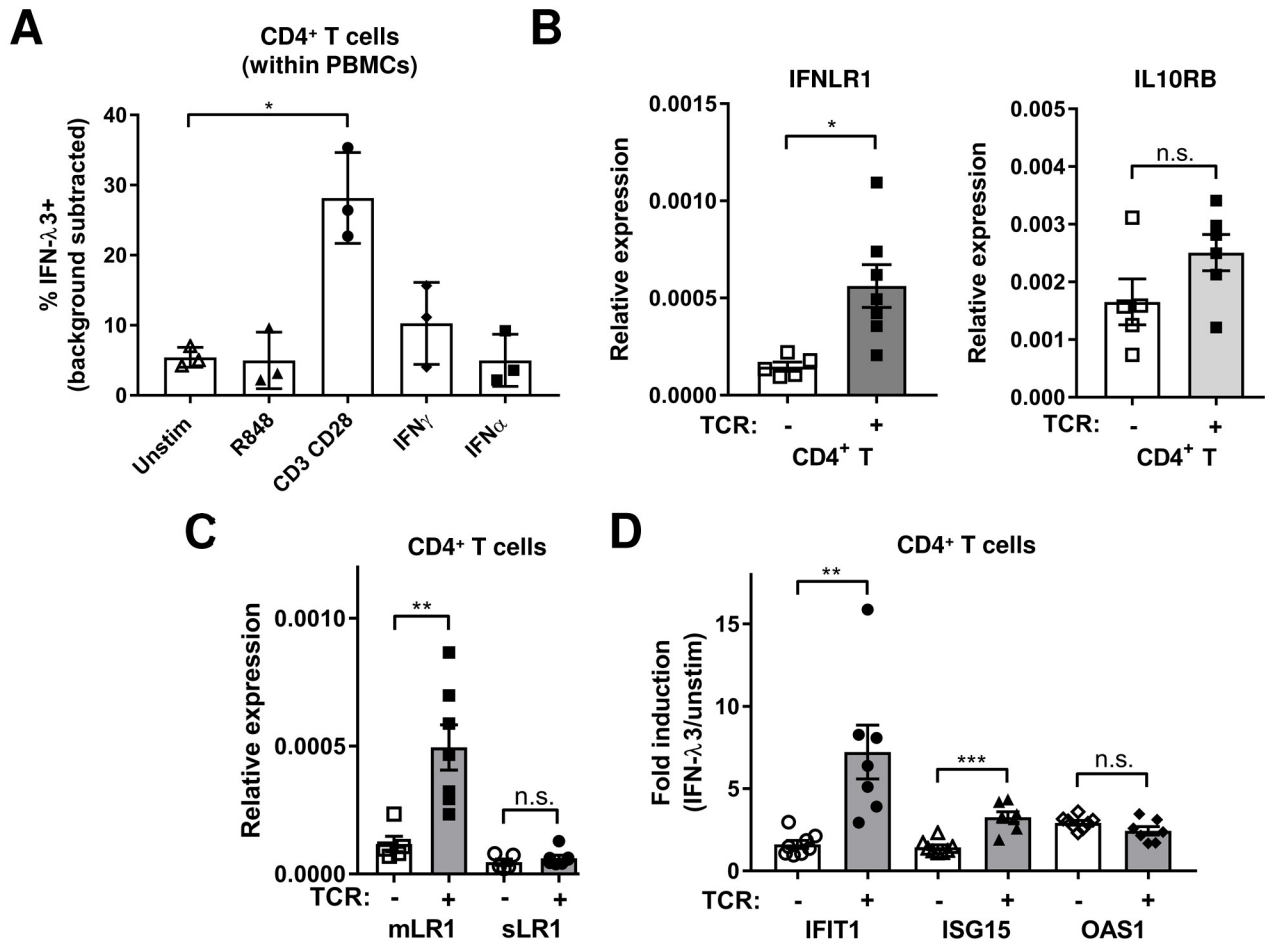


Fig 6. TCR stimulation upregulates IFN-λ3 binding and IFN-λR1 expression leading to greater ISG induction in CD4⁺ T cells. A) IFN-λ3 (5 μg/ml) binding to LIVE/DEAD⁻ CD4⁺ T cells within total PBMCs that had been cultured for 3 days in either media only (unstimulated (unstim)), or with the following stimuli: R848 (1 μg/ml), anti-CD3 (plate bound 1.5 μg/ml) and soluble anti-CD28 (1 μg/ml), IFN-γ (10 ng/ml) or IFN-α2 (1000 IU/ml). B-C) Total *IFNLR1*, *IL10RB* (B), full length membrane (*mLR1*) or soluble (*sLR1*) *IFNLR1* variant (C) transcript expression in CD4⁺ T cells sorted after 3 days of PBMC culture with or without anti-CD3/anti-CD28 stimulation (TCR). D) ISG induction in sorted CD4⁺ T cells treated with IFN-λ3 (100 ng/ml) for 24 hrs after sorting from PBMCs which had previously been cultured in unstimulated or anti-CD3/anti-CD28 stimulated (TCR) conditions for 3 days. Fold induction of 3 ISGs are shown. Graphs show means +/- SD (A) or SEM (B-D) with each symbol representing a different healthy individual. All RT-qPCR results are normalized to *B2M* reference gene. n.s., not significant, *, P<0.05, **, P<0.01, ***, P<0.001, one-way ANOVA, Dunnett's multiple comparison test comparing to unstimulated (A), unpaired t-test (B-D).

<https://doi.org/10.1371/journal.ppat.1008515.g006>

bind and respond to IFN-λ3 in human peripheral blood, and demonstrate that a unique soluble IFN-λR1 variant present in higher primates inhibits IFN-λ3-mediated ISG induction by binding the cell surface and sequestering IFN-λ3 away from a functional membrane spanning IFN-λR heterodimer complex. Activation of immune cells promotes specific *mIFNLR1* expression and the direct interaction of IFN-λ3 with CD4⁺ T cells induces an antiviral state to decrease HIV-1 infection. Thus, unlike in mice, type III IFNs have the potential to directly impact resting and activated human adaptive immune cells.

Quantification of cell surface IFN-λ3 binding to peripheral blood immune cells correlated with *IFNLR1* transcript expression in most cases. Human B and T cells can interact directly with IFN-λ3, and IFN-λ3 binding levels correlated with the magnitude of ISG induction in stimulation assays. Consistent with previous literature, human monocytes and NK cells did not respond directly to type III IFNs [35, 39, 61]. However, there were exceptions where IFN-

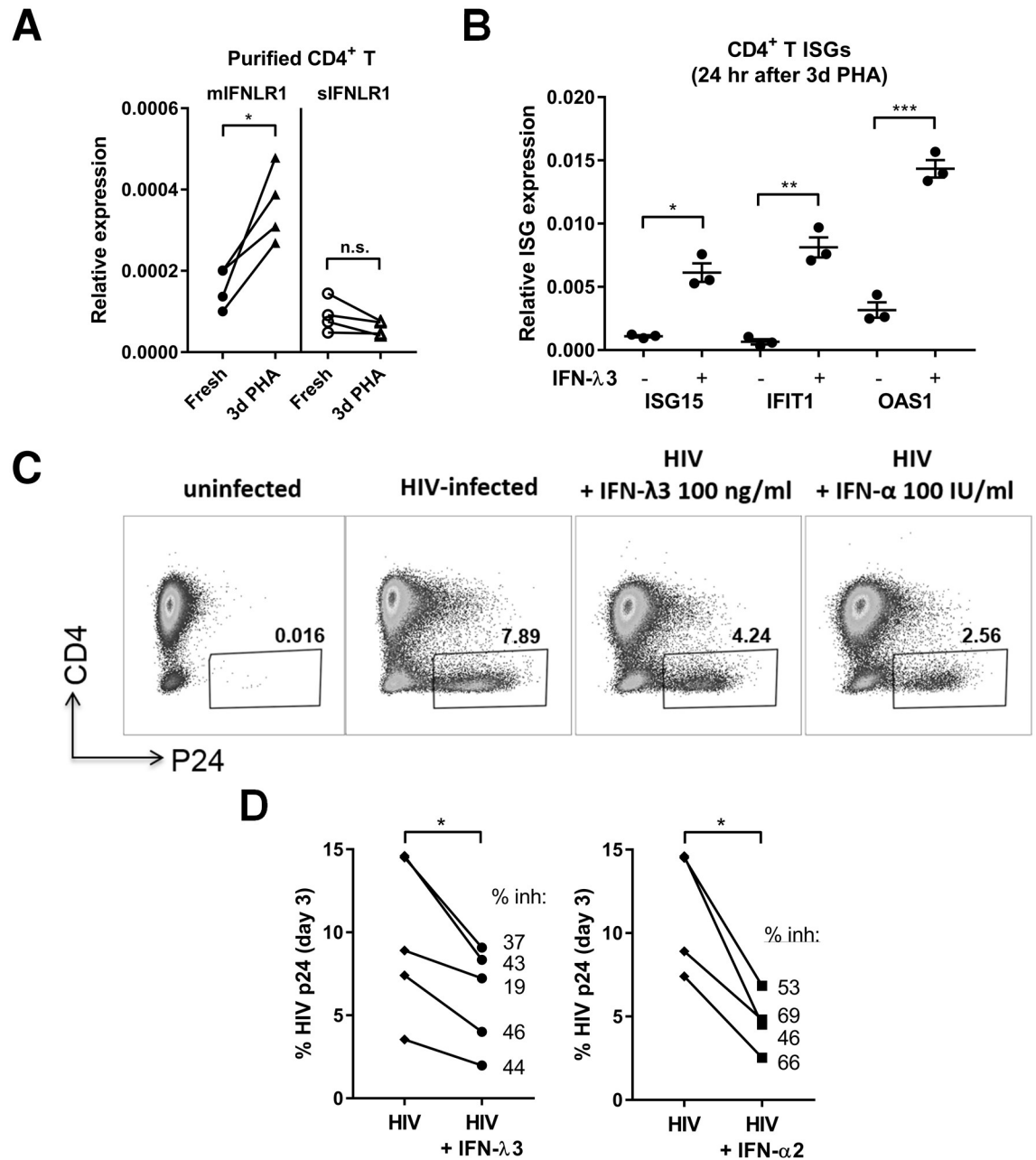


Fig 7. IFN-λ3 inhibits HIV-1 infection of purified CD4⁺ T cells. A) Relative expression of full length, membrane (*mIFNLR1*) and small, soluble (*sIFNLR1*) variant expression in purified CD4⁺ T cells on day 0 or day 3 after PHA stimulation (normalized to *B2M* reference gene). B) ISG (*ISG15*, *IFIT1*, *OAS1*) expression in purified CD4⁺ T cells cultured with or without IFN-λ3 (100 ng/ml) for 24 hrs after 3 days of PHA stimulation. Results are shown as means \pm SD. C-D) Quantification of HIV-1 infection via p24 intracellular flow cytometry. C) Representative p24 staining from 1 healthy individual for all treatments tested. D) % HIV-1 p24 staining from 4–5 different individuals for HIV-1 infection alone compared to cells pre-treated with IFN-λ3 (100 ng/ml) or IFN-α2 (100 IU/ml). Symbols represent means from duplicate wells per individual with each symbol representing a different healthy blood donor. *, $P < 0.05$, **, $P < 0.01$, ***, $P < 0.001$, paired t-tests.

<https://doi.org/10.1371/journal.ppat.1008515.g007>

λ3 binding did not match *IFNLR1* transcript expression and/or ISG induction. We noted that liver and lung epithelial cells expressed similar or lower total *IFNLR1* mRNA than B cells, but bound ~5-fold more IFN-λ3 and upregulated ISGs up to 50-fold greater than B cells. Upon further analysis of the variants of *IFNLR1*, we found every immune cell isolated expressed

greater *sIFNLR1* transcripts relative to *mIFNLR1*, compared to epithelial cells. sIFN- λ R1 bound well to every cell type tested, and surprisingly promoted increased binding of IFN- λ 3 to the cell surface. Significant inhibition of ISG induction in the presence of sIFN- λ R1 likely occurs because the IFN- λ 3-sIFN- λ R1 complex could not initiate signaling due to the lack of cytoplasmic tail in sIFN- λ R1. The lower baseline expression of *sIFNLR1* in epithelial cells, may also be the reason that sIFN- λ R1 bound 100% of epithelial cells at a 10–100 fold lower dose than immune cells. Our data add to the understanding of IFN- λ -mediated pathogen control mechanisms by the expression of sIFN- λ R1 only in upper primates, and mIFN- λ R1 upregulation upon activation of B cells, CD4⁺ T cells, and neutrophils. The presence of the human sIFN- λ R1 variant was detected at the time of receptor discovery in 2003 [3, 4], and a previous report indicated pre-incubation of sIFN- λ R1 with IFN- λ 1 decreased stimulation of a hepatocyte cell line [35], however no mechanisms that changed the relative expression of the 2 main splice forms of IFN- λ R1 have been investigated. Soluble cytokine receptors can have either inhibitory or enhancing properties. For example, IL-22BP, also an IL-10 cytokine family member, acts as a decoy blocking IL-22 binding at mucosal surfaces where IL-22R is expressed [62, 63]. In contrast, sIFN- α 2a binding to IFN- α enhances IFN- α responses *in vivo* [64]. It is unclear why primitive primates and lower mammals do not have evidence of sIFN- λ R1 expression, while both mice and humans express IL-22BP and sIFN- α 2a. Compared to type I IFNs, type III IFNs induce a slower, lower magnitude response [23, 24] with less inflammatory effects in human clinical trials or in mouse lung infections [25, 65–67]. The expression of sIFN- λ R1 may have evolved as a mechanism to contribute to immune cells remaining in an “off” condition until they receive optimal activation signals to allow for increased type III IFN responses, unlike all immune cells responding to type I IFNs at baseline. Since our work identified stimuli that regulate mIFN- λ R1, but not sIFN- λ R1 expression, determining what stimuli modulate sIFN- λ R1 expression will be of future interest.

We observed IFN- λ 3 bound well to monocytes despite very little *mIFNLR1* transcript expression, but ISGs were not induced in our assays. The binding was not an artifact of the 6 His-tag on IFN- λ 3, since an unrelated, similarly tagged protein did not bind monocytes. IFN- λ 3 is not likely binding IL-10RB alone, or high binding would have also been observed to neutrophils, which also express very high levels of IL-10RB. In addition, the affinity of type III IFNs to IL-10RB alone is very low [68]. Since we showed that recombinant sIFN- λ R1 directly binds monocytes, we speculate that IFN- λ 3 binds monocytes in our assay at least in part because sIFN- λ R1 is already bound to the cell surface. Altogether, our data indicate there are multiple layers of regulation of the responses to IFN- λ 3.

While many studies have demonstrated potent antiviral activity of type III IFNs at epithelial barrier sites, much less is known regarding type III IFN antiviral activity in peripheral blood. Previous studies proposed that human and mouse T cells do not directly respond to IFN- λ s, and that IFN- λ dependent regulatory effects occur via a specific subset of DCs or neutrophils [20, 25, 35, 44, 69–71]. Here, we show for the first time that human CD8⁺ T cells express significantly greater *IFNLR1* transcripts, and bind IFN- λ 3 to a higher degree than CD4⁺ T cells, leading to the upregulation of ISGs in response to IFN- λ 3 *in vitro*. Only upon TCR or PHA activation of CD4⁺ T cells, did the level of *IFNLR1* mRNA expression match or surpass that seen in CD8⁺ T cells, in turn leading to greater ISG induction and ultimately inhibition of HIV-1 infection by IFN- λ 3 treatment. While two previous studies found IFN- λ 1 or IFN- λ 2 could inhibit or enhance HIV-1 infection of CD4⁺ T cells [72, 73], our findings support the IFN- λ 3-mediated induction of an antiviral program in CD4⁺ T cells, with no indication of an enhancement of infection. Our data demonstrate that CD4⁺ and CD8⁺ T cells can be directly regulated by type III IFNs to combat viral infections. While we focused on IFN- λ 3 activity in

this study, we predict other IFN- λ family members would be able to stimulate ISGs in the same cell types since they all bind the same receptor, but receptor affinity may affect the magnitude of the response [74].

Our results that human neutrophils bind low levels of IFN- λ 3 and express low levels of IFN- λ R1 are in contrast to mouse models of influenza virus or *Aspergillus fumigatus* infection and arthritis or colitis where mouse neutrophils directly respond to IFN- λ to modulate responses [19, 20, 25, 46]. Limited data has been published measuring ISG induction by IFN- λ s in human neutrophils. Human neutrophils responded ~20-fold less than mouse neutrophils to IFN- λ 2 [20], and IFIT1 was not induced in human neutrophils after IFN- λ 1 treatment [75]. IFN- λ 3 may induce greater ISG levels in neutrophils *in vivo* because neutrophils survive longer than the 5 hour time point used in the current study. Additionally, whether human neutrophils are also regulated by the unique STAT-1 independent, non-translational signaling pathway seen after Ifn- λ 2 treatment of mouse neutrophils is unclear [20]. Our quantification showing that human neutrophils express low levels of *IFNLR1* transcripts directly *ex vivo* are in agreement with a published human microarray and single cell RNA sequencing results [54, 55]. Subsequent stimulation of neutrophils with TLR agonists and bacteria induced *IFNLR1* mRNA expression, which complements data showing that *Aspergillus fumigatus* addition to neutrophils upregulated IFN- λ R1 expression [46]. Therefore, human neutrophils may optimally respond to IFN- λ s *in vivo* through upregulation of IFN- λ R1 during inflammatory conditions. Future work directly measuring IFN- λ R1 protein on the cell surface after stimulations will only be possible when a specific, sensitive antibody becomes available.

There is a growing list of differences between the mouse and human type III IFN system. Mice only have functional *Ifnl2* and *Ifnl3* genes, and here we show the sIFN- λ R1 splice variant is not present in mice and other non-primates. Although initial studies found human B cells do not respond to IFN- λ s [35, 39], we and another group have now clearly demonstrated human B cells directly respond to IFN- λ 3 (current study) and IFN- λ 1 [45]. Our data showing IFN- λ 3 binds to human pDCs matches previous studies showing human pDCs respond to type III IFNs [41, 43, 44], but studies have found contradicting results for whether type III IFNs stimulate ISGs in mouse pDCs [7, 20]. We showed that activation through TCR, BCR, or TLRs upregulated *IFNLR1* mRNA expression and IFN- λ 3 binding to multiple human immune cell types, but a recent study found TLR3 stimulation or addition of Sendai virus did not upregulate *IFNLR1* transcript expression in a hepatocyte cell line [26]. Therefore, *IFNLR1* expression may be differentially regulated in epithelial cells compared to immune cells. Interestingly, we found IFN- α 2 decreased IFN- λ 3 binding to B cells, whereas a previous study demonstrated IFN- α treatment upregulates *IFNLR1* mRNA expression in hepatocytes [9]. IFN- γ treatment alone was also unable to upregulate IFN- λ R1 expression in B cells or T cells. Our findings demonstrate IFN- λ R1 expression is uniquely regulated in immune cells compared to epithelial cells, and future work should confirm if IFN- λ R1-dependent regulatory mechanisms discovered in mouse models are reproducible in human studies.

In summary, our study has provided clear evidence of which human immune cells express functional IFN- λ R with major differences in IFN- λ R1 expression between mice and humans, especially within the adaptive immune system. The remarkable absence of IFN- λ R1 expression in most mouse immune cells begs the question for how phenotypes and immunoregulatory mechanisms could differ during a viral infection or autoimmune mouse model if IFN- λ R1 cell expression mimicked that seen in humans. Going forward, studying the regulation of human IFN- λ R1 expression in epithelial cells and immune cells will provide critical information to guide mechanistic studies related to type III IFN

regulation of immune responses, with the goal of developing therapies to fight viruses, dampen chronic inflammation at mucosal sites, and treat cancer with less side effects compared to type I IFNs.

Materials and methods

Ethics statement

This study was approved by the University of Alberta Health Research Ethics Board (Pro00046564). All blood donors gave written informed consent in accordance with the Declaration of Helsinki. Normal human lungs that were not used for transplantation were obtained via a tissue retrieval service (International Institute for the Advancement of Medicine, Edison, NJ). The identity of donors was not provided, although basic demographic data was included. Ethical approval to obtain normal human bronchial epithelial cells (NHBE) was obtained from the Conjoint Health Research Ethics Board of the University of Calgary and from the Internal Ethics Board of the International Institute for the Advancement of Medicine.

Cell lines and primary cell isolation

Huh7.5 cells (from Dr. Charles Rice, The Rockefeller University) and Huh7 IFNLR1 knockout cells [49] (from Dr. Ram Savan, University of Washington), were cultured in DMEM containing: 10% fetal bovine serum (FBS), 100 U/ml penicillin, 100 µg/ml streptomycin, 1X MEM non-essential amino acids and 4 mM L-glutamine (media from GE Healthcare, supplements from ThermoFisher). BEAS-2B and DG75 cells were obtained from ATCC and cultured using the BEGM bronchial epithelial growth medium Bulletkit (Lonza) according to the manufacturer's instructions, except hydrocortisone was not added to medium during any cytokine stimulations. PBMCs were isolated from healthy human individuals by Ficoll-Paque PLUS (GE Healthcare) gradient centrifugation. All PBMC experiments used freshly isolated cells. Immune cells were sorted using a BD FACSAria III cell sorter within a biosafety cabinet with dead cells excluded using LIVE/DEAD Near IR (ThermoFisher) after gating out doublets. Cells were sorted as follows: B cells: CD20⁺CD3⁻CD56⁻CD14⁻, CD4⁺ T cells: CD3⁺CD4⁺CD8⁻, CD8⁺ T cells: CD3⁺CD8⁺CD4⁻, Monocytes: CD14⁺CD3⁻CD20⁻, NK cells: CD56⁺CD3⁻. Purities were routinely ≥ 97–99% and pDCs were not detectable by flow cytometry (CD123⁺HLA-DR⁺). Representative purity results are shown in S5 Fig. In some experiments, B cells were isolated with a negative B cell isolation kit (StemCell Technologies) or CD14⁺ monocytes were isolated by CD14 positive selection (Miltenyi Biotec), but results were comparable whether cells were isolated via FACS or magnetic selection. PBMCs or isolated immune cells were cultured in RPMI 1640 containing: 10% FBS, 100 U/ml penicillin, 100 µg/ml streptomycin, 10 mM HEPES and 2 mM glutamax (media from GE Healthcare, supplements from ThermoFisher). Primary human hepatocytes were purchased from BioreclamationIVT. Normal, nontransplanted human lungs were obtained via a tissue retrieval service (International Institute for the Advancement of Medicine, Edison, NJ). Bronchial epithelial cells were isolated as previously described [76], and cultured in BEGM with supplements (Lonza) as previously described [77]. In brief, cells were plated in 6 or 12 well plates and utilized at ~70% confluence (typically after 10–11 days with media change every 2 days) for binding or stimulation assays. Neutrophils were isolated from healthy donor whole blood with Polymorphprep (Axis Shield) according to the manufacturer's protocol to achieve highly pure, unprimed neutrophils suitable for gene expression studies [78]. Purities were ≥ 95% (S2 Fig) and pDCs were not detectable by flow cytometry. IFN-λ3 binding to neutrophils was also quantified after RBC magnetic depletion (StemCell Technologies). All cells were maintained in an incubator with a humidified atmosphere with 5% CO₂ at 37°C.

Flow cytometry

The IFN- λ 3 binding assay was performed as published [48]. In brief, cells were cultured with or without His-tagged IFN- λ 3 (R&D Systems) diluted in PBS containing 1% BSA on ice for 60 min at indicated doses. In some experiments, recombinant sIFN- λ R1 or IL-10RB protein (R&D Systems) was added simultaneously with IFN- λ 3 while Fc γ Rs were blocked with 150 μ g/ml human IgG (Jackson ImmunoResearch) or human Fc Block (BD Biosciences). Cells were then washed (PBS + 1% BSA + 0.05% sodium azide) and stained with anti-His PE (Miltenyi Biotec) in combination with multiple surface marker antibodies on ice for 40 min in the dark. Anti-His PE secondary antibody was added alone in a parallel sample to obtain background fluorescence that was subtracted from each sample ('background subtracted'), and background was always less than 1%. Cells were washed again and re-suspended in 2% paraformaldehyde (Electron Microscopy Sciences) at room temperature for 15 min in the dark. Paraformaldehyde was washed away prior to analysis. sIFN- λ R1-Fc or IL-10RB-Fc (R&D Systems) binding to the cell surface was similarly quantified. sIFN- λ R1 or IL-10RB was added to cells for 45 min on ice and after washing, anti-Fc PE (Biolegend) was added to detect receptor bound to the cell surface. anti-Fc PE antibody was always added alone in a parallel sample so that any background would be subtracted. The following antibodies were used to identify our subpopulations: CD3 (clone UCHT1 Biolegend), CD4 (clone SK3 BD Bioscience, RPA-T4 eBioscience), CD8 (clone SK1 Biolegend), CD14 (clone HCD14 Biolgend, 61D3 eBioscience), CD56 (clone HCD56 Biolegend), CD20 (clone 2H7 Biolegend), CD66b (clone G10F5 Biolegend), HLA-DR (clone L243 eBioscience), CD123 (clone 6G6 eBioscience), CD11c (clone Bu15 Biolegend), CD16 (clone 3G8 Biolegend), IgD (clone IA6-2 Biolegend), CD27 (clone O323 Biolegend). For each antibody panel, a dump channel, where antibodies to multiple immune cells not of interest for that assay, was used to exclude contaminating cell types. Examples of our gating strategy are shown in S1 and S2 Figs. For stimulation experiments, LIVE/DEAD Near IR (ThermoFisher) was utilized within the dump gate to determine live cells for IFN- λ 3 binding quantification. NHBE and hepatocytes were incubated with IFN- λ 3 in the same binding assay without any surface staining antibodies since they were pure populations. Samples were analyzed using a BD LSR Fortessa X-20 or LSR Fortessa-SORP Flow Cytometer (5 laser: 375 nm, 405 nm, 488 nm, 561 nm, and 633 nm) and FlowJo software (BD Biosciences) was used for data analysis and graph generation. In certain experiments, sIFN- λ R1 binding was also visualized via imaging cytometry using the Amnis ImageStream[®]X mark II Flow Cytometer (Millipore-Sigma) and Inspire[®] (Amnis) software. 6,000–12,000 total events were collected for each experiment. Samples were imaged at 60x magnification and IDEAS[®] (Amnis) software was used for single cell analysis.

Real-time reverse transcription PCR (RT-qPCR)

PBMCs or sorted immune cell subsets (2×10^6 cells/ml) or NHBE (6 well plate, 70% confluence) were incubated at 37°C with or without IFN- λ 3 (100 ng/ml) or other stimuli for the time points indicated. Stimuli tested in this study include: IFN- λ 3 (R&D Systems), IFN- α 2b (INTRON[®] A, Merck), recombinant IFN- λ R1 and IL-10RB (R&D Systems), R848 (InvivoGen), anti-CD3 (clone HIT3a) and anti-CD28 (clone CD28.2) were from Biolegend. Anti-IgM, IgG, IgA (Jackson ImmunoResearch), anti-CD40 (R&D Systems), IFN- γ (Peprotech). Heat killed *Listeria monocytogenes* 10403S supernatant was prepared as described [79]. Cells were then washed with PBS and the pellet was resuspended in TRIzol (ThermoFisher). For quantifying *IFNLR1* and *IL10RB* transcripts directly *ex vivo*, sorted cells were resuspended in TRIzol without incubation. All samples were stored at -80°C. Total RNA was extracted with Direct-zol mini or micro RNA isolation kits (Zymo Research) in accordance with manufacturer's

guidelines, with on column DNase I digestion. Reverse transcription was performed with a Superscript VILO IV mastermix (ThermoFisher). RT-qPCR was performed with a Bio-Rad CFX 96 using ThermoFisher POWER SYBR mastermix (ThermoFisher) according to the manufacturer's protocol: 95°C for 10 min, and then repeating 40 times, 95°C for 15 sec and 60°C for 60 sec, followed by a melting curve analysis. SYBR green primer sequences are listed in [S4 Table](#), with the exception of the *B2M* QuantiTect Primers (Qiagen). For Taqman analysis of *IFNLR1* (Hs00417120_m1), *IL10RB* (Hs00175123_m1), *HPRT1* (Hs02800695_m1), *RPL13A* (Hs04194366_g1) and *B2M* (Hs99999907_m1) (ThermoFisher), Taqman Fast Advanced mastermix (ThermoFisher) was used with the following cycling parameters: 50°C for 2 min, 95°C for 2 min, and then repeating 40 times, 95°C for 1 sec and 60°C for 20 sec. No template controls were run for every set of primers on each plate. Samples were normalized to the geometric mean of two reference genes, *HPRT1* and *RPL13A*, as described [80], unless indicated when *B2M* was the reference gene that was stably expressed between samples. Fold changes in mRNA expression were calculated using the $\Delta\Delta C_t$ method with comparisons of stimulated to unstimulated cells. Relative expression values were calculated by $2^{-\Delta C_t}$ after normalization to reference genes indicated.

CD4⁺ T cell HIV-1 infection

CD4⁺ T cells were isolated using a CD4⁺ T cell enrichment kit (StemCell Technologies) according to manufacturer's instructions. The enriched CD4⁺ T cells (2×10^6 cells/ml) were maintained in RPMI 1640 media supplemented with 10% FBS, 100 U/ml penicillin, 100 µg/ml streptomycin, 10 µg/ml phytohemagglutinin-M (PHA-M; Sigma), and 50 U/ml recombinant IL-2 at 37°C and 5% CO₂ incubator for 3 days. Excess PHA was removed by washing with fresh media and cell density was adjusted to 7×10^5 cells/ml in 48 well plates. Activated T cells were cultured with media alone, IFN- α 2 (100 IU/ml) or IFN- λ 3 (100 ng/ml) for 24 hours before CXCR4-tropic HIV-1 LAI virus (AIDS Research and Reagent Program, NIH) infection via magnetofection (OZ Biosciences), as previously described [81]. Non-bound, excess HIV-1 virus was washed away after 24 hrs of infection and fresh media with or without IFNs were added back for an additional 2 days in culture. Uninfected and infected CD4⁺ T cells with or without IFN- λ 3 treatment were stained intracellularly with HIV-1 KC57-p24 core (Beckman Coulter) antibody on day 3 post HIV-1 infection.

Statistics and data analysis

Graphs were formulated and data were analyzed in Graphpad Prism 7 or FlowJo software (BD Biosciences). A P-value less than 0.05 was considered significant. The number of healthy donors or replicates and statistical tests are specified in each figure legend.

Supporting information

S1 Fig. Flow cytometry gating strategy. A) Gating total cells and removing any doublets. B-H) Outline of gating strategy for B cells (B), monocytes (C), natural killer (NK) cells (D), plasmacytoid dendritic cells (pDCs) (E), CD4⁺ T cells (F), myeloid DCs (mDCs) (G) and CD8⁺ T cells (H). Dump refers to multiple antibodies labeled with same fluorophore added to exclude other subsets (eg. Dump gate for B cells: antibodies to CD3, CD14, CD56 and CD16). (TIF)

S2 Fig. Flow cytometry gating strategy for freshly isolated neutrophils. Neutrophils purified with Polymorphprep gradient centrifugation were identified as CD66b⁺ CD16⁺ after gating by size and gating out T cells (CD3), B cells (CD20) and monocytes (CD14). Purities were

routinely >95–99%.
(TIF)

S3 Fig. Epithelial cells bind greater levels of IFN- λ 3 than immune cells, results are reproducible over time, and IFN- λ 3 binding requires *IFNLR1* expression. A-B) IFN- λ 3 binding was quantified via flow cytometry as described in the Materials and methods. A) Fold increase in median PE binding after adding 1 or 5 μ g/ml IFN- λ 3 to epithelial cells (NHBE or hepatocytes (hep)) or total human PBMCs with gating on B cells, monocytes (mono), pDCs or mDCs. Graph shows mean \pm SD for 3 (hep), 5 (NHBE), 8–14 (1 μ g/ml immune cell) or 21–22 (5 μ g/ml immune cell) different donors. B) The % IFN- λ 3+ cells quantified for monocytes (mono) or B cells from our binding assay repeated on the same healthy individual at least 6 months apart. C) Binding percentages to CD3⁺ T cells as detected by flow cytometry for IFN- λ 3 or a control protein that was similarly his-tagged (OBCAM) where means \pm SD are shown. Each symbol represents a different individual. D) IFN- λ 3 binding to Huh7 *IFNLR1* knockout cells compared to adding the secondary antibody alone. Data are representative of 2 independent experiments.

(TIF)

S4 Fig. IFN- λ 3 binding levels significantly correlate between specific immune cell subsets. Pearson correlation coefficients (r) calculated when comparing IFN- λ 3 percent binding to immune cell subsets where each symbol is a different healthy individual.

(TIF)

S5 Fig. Purity of cells after sorting. Representative flow cytometry plots of cells acquired after sorting checking the purity of the populations we used for RT-qPCR.

(TIF)

S6 Fig. Baseline ISG expression and IFN- α 2 mediated ISG induction in purified primary human cells. A) Baseline (untreated) expression levels of *ISG15*, *IFIT1* and *OAS1* in isolated cell types. B) RT-qPCR quantification of *ISG15*, *IFIT1*, and *IFI44* induced after addition of positive control IFN- α 2 (1000 IU/ml (neutrophil), 100 IU/ml (monocyte, B cell, CD4⁺ or CD8⁺ T cells)) to purified cells. Neutrophils were treated for 5 hrs, all other cell types were treated for 24 hrs. Graphs show relative expression (A) or fold induction relative to unstimulated negative control (B) after normalization to the geomean of *HPRT1* and *RPL13A* reference genes. Bars represent mean \pm SEM from 4–6 (B, T cell), 3–4 (monocyte), 4–6 (neutrophil) or 5 normal human bronchial epithelial cell (NHBE) different donors. *, $P < 0.05$, **, $P < 0.01$, ***, $P < 0.001$, ****, $P < 0.0001$, one-way ANOVA, Tukey's multiple comparisons test where significant comparisons to monocytes (mono, m) and neutrophils (neut, n) are shown (A). All other comparisons were not significant.

(TIF)

S7 Fig. Soluble IFN- λ R1 directly binds to Huh7.5 cells and enhances IFN- λ 3 binding. A) Quantification of recombinant sIFN- λ R1 (0.01, 0.1 μ g/ml) binding to Huh7.5 cells with or without IFN- λ 3 (100 ng/ml). B) IFN- λ 3 binding to Huh7.5 cells where IFN- λ 3 (0.1 μ g/ml) was added with or without sIFN- λ R1 (0.1, 1 μ g/ml) or IL-10RB (1 μ g/ml). C) IFN- λ 3 (0.25 μ g/ml) binding to Huh7.5 cells when added alone or with sIFN- λ R1 (0.5 μ g/ml) added either simultaneously or sIFN- λ R1 was added first for 45 min on ice before cells were washed twice and then IFN- λ 3 added. A-C) Histograms are representative of 2–3 independent experiments. 2nd antibody (Ab) alone is negative control to show background fluorescence: A) anti-Fc PE alone, B-C) anti-his PE alone.

(TIF)

S1 Table. Statistical analyses comparing IFN- λ 3 binding between immune cell subsets and NHBE. 5 μ g/ml IFN- λ 3 binding results were compared in 3–22 different individuals. One-way ANOVA with Tukey's multiple comparisons. n.s. = not significant, *, $P < 0.05$, **, $P < 0.01$, ***, $P < 0.001$, ****, $P < 0.0001$. Data relates to [Fig 1D](#).
(DOCX)

S2 Table. Correlation coefficients of percent IFN- λ 3 binding between immune cell subsets. Pearson correlation coefficients (P value result in brackets, n.s. = not significant, *, $P < 0.05$, ***, $P < 0.001$) calculated from 5 μ g/ml IFN- λ 3 binding results from 11–18 different individuals.
(DOCX)

S3 Table. Evidence for the presence of a small/soluble variant of *IFNL1* across multiple species.
(DOCX)

S4 Table. List of SYBR RT-qPCR primer sequences.
(DOCX)

Acknowledgments

We thank members of the Houghton and Tyrrell laboratories for their insights and helpful discussions, and Dr. Charles Rice and Dr. Ram Savan for providing essential cell lines for this work. We also thank staff at the University of Alberta Faculty of Medicine & Dentistry Flow Cytometry Facility, which receives financial support from the Faculty of Medicine & Dentistry and Canada Foundation for Innovation (CFI) awards to contributing investigators.

Author Contributions

Conceptualization: Deanna M. Santer, Michael Joyce, Michael Houghton.

Funding acquisition: Michael Houghton.

Investigation: Deanna M. Santer, Gillian E. S. Minty, Dominic P. Golec, Julia Lu, Julia May, Afshin Namdar, Juhi Shah.

Methodology: Deanna M. Santer, Afshin Namdar, Shokrollah Elahi, David Proud.

Resources: Shokrollah Elahi, David Proud, D. Lorne Tyrrell.

Supervision: Deanna M. Santer, Michael Houghton.

Validation: Deanna M. Santer.

Writing – original draft: Deanna M. Santer, Gillian E. S. Minty, Michael Joyce.

Writing – review & editing: Deanna M. Santer, Gillian E. S. Minty, Dominic P. Golec, Julia Lu, Julia May, Afshin Namdar, Juhi Shah, Shokrollah Elahi, David Proud, Michael Joyce, D. Lorne Tyrrell, Michael Houghton.

References

1. Isaacs A, Lindenmann J. Virus interference. I. The interferon. *Proc R Soc Lond B Biol Sci.* 1957; 147 (927):258–267. <https://doi.org/10.1098/rspb.1957.0048> PMID: 13465720
2. Kotenko SV, Gallagher G, Baurin VV, Lewis-Antes A, Shen M, Shah NK, et al. IFN-lambdas mediate antiviral protection through a distinct class II cytokine receptor complex. *Nat Immunol.* 2003; 4(1):69–77. <https://doi.org/10.1038/ni875> PMID: 12483210

3. Sheppard P, Kindsvogel W, Xu W, Henderson K, Schlutsmeyer S, Whitmore TE, et al. IL-28, IL-29 and their class II cytokine receptor IL-28R. *Nat Immunol*. 2003; 4(1):63–68. <https://doi.org/10.1038/ni873> PMID: 12469119
4. Dumoutier L, Lejeune D, Hor S, Fickenscher H, Renauld JC. Cloning of a new type II cytokine receptor activating signal transducer and activator of transcription (STAT)1, STAT2 and STAT3. *Biochem J*. 2003; 370(Pt 2):391–396. <https://doi.org/10.1042/BJ20021935> PMID: 12521379
5. Prokunina-Olsson L, Muchmore B, Tang W, Pfeiffer RM, Park H, Dickensheets H, et al. A variant upstream of IFNL3 (IL28B) creating a new interferon gene IFNL4 is associated with impaired clearance of hepatitis C virus. *Nat Genet*. 2013; 45(2):164–171. <https://doi.org/10.1038/ng.2521> PMID: 23291588
6. Egli A, Santer DM, O'Shea D, Tyrrell DL, Houghton M. The impact of the interferon-lambda family on the innate and adaptive immune response to viral infections. *Emerg Microbes Infect*. 2014; 3(7):e51. <https://doi.org/10.1038/emi.2014.51> PMID: 26038748
7. Ank N, Iversen MB, Bartholdy C, Staeheli P, Hartmann R, Jensen UB, et al. An important role for type III interferon (IFN-lambda/IL-28) in TLR-induced antiviral activity. *J Immunol*. 2008; 180(4):2474–2485. <https://doi.org/10.4049/jimmunol.180.4.2474> PMID: 18250457
8. Ank N, West H, Bartholdy C, Eriksson K, Thomsen AR, Paludan SR. Lambda interferon (IFN-lambda), a type III IFN, is induced by viruses and IFNs and displays potent antiviral activity against select virus infections in vivo. *J Virol*. 2006; 80(9):4501–4509. <https://doi.org/10.1128/JVI.80.9.4501-4509.2006> PMID: 16611910
9. Duong FH, Trincucci G, Boldanova T, Calabrese D, Campana B, Krol I, et al. IFN-lambda receptor 1 expression is induced in chronic hepatitis C and correlates with the IFN-lambda3 genotype and with nonresponsiveness to IFN-alpha therapies. *J Exp Med*. 2014; 211(5):857–868. <https://doi.org/10.1084/jem.20131557> PMID: 24752298
10. Hou W, Wang X, Ye L, Zhou L, Yang ZQ, Riedel E, et al. Lambda interferon inhibits human immunodeficiency virus type 1 infection of macrophages. *J Virol*. 2009; 83(8):3834–3842. <https://doi.org/10.1128/JVI.01773-08> PMID: 19193806
11. Lazear HM, Daniels BP, Pinto AK, Huang AC, Vick SC, Doyle SE, et al. Interferon-lambda restricts West Nile virus neuroinvasion by tightening the blood-brain barrier. *Sci Transl Med*. 2015; 7(284):284ra259.
12. Mahlakoiv T, Hernandez P, Gronke K, Diefenbach A, Staeheli P. Leukocyte-derived IFN-alpha/beta and epithelial IFN-lambda constitute a compartmentalized mucosal defense system that restricts enteric virus infections. *PLoS Pathog*. 2015; 11(4):e1004782. <https://doi.org/10.1371/journal.ppat.1004782> PMID: 25849543
13. Mordstein M, Kochs G, Dumoutier L, Renauld JC, Paludan SR, Klucher K, et al. Interferon-lambda contributes to innate immunity of mice against influenza A virus but not against hepatotropic viruses. *PLoS Pathog*. 2008; 4(9):e1000151. <https://doi.org/10.1371/journal.ppat.1000151> PMID: 18787692
14. Mordstein M, Neugebauer E, Ditt V, Jessen B, Rieger T, Falcone V, et al. Lambda interferon renders epithelial cells of the respiratory and gastrointestinal tracts resistant to viral infections. *J Virol*. 2010; 84(11):5670–5677. <https://doi.org/10.1128/JVI.00272-10> PMID: 20335250
15. Nice TJ, Baldrige MT, McCune BT, Norman JM, Lazear HM, Artyomov M, et al. Interferon-lambda cures persistent murine norovirus infection in the absence of adaptive immunity. *Science*. 2015; 347(6219):269–273. <https://doi.org/10.1126/science.1258100> PMID: 25431489
16. Ge D, Fellay J, Thompson AJ, Simon JS, Shianna KV, Urban TJ, et al. Genetic variation in IL28B predicts hepatitis C treatment-induced viral clearance. *Nature*. 2009; 461(7262):399–401. <https://doi.org/10.1038/nature08309> PMID: 19684573
17. Tanaka Y, Nishida N, Sugiyama M, Kurosaki M, Matsuura K, Sakamoto N, et al. Genome-wide association of IL28B with response to pegylated interferon-alpha and ribavirin therapy for chronic hepatitis C. *Nat Genet*. 2009; 41(10):1105–1109. <https://doi.org/10.1038/ng.449> PMID: 19749757
18. Thomas DL, Thio CL, Martin MP, Qi Y, Ge D, O'Huigin C, et al. Genetic variation in IL28B and spontaneous clearance of hepatitis C virus. *Nature*. 2009; 461(7265):798–801. <https://doi.org/10.1038/nature08463> PMID: 19759533
19. Blazek K, Eames HL, Weiss M, Byrne AJ, Perocheau D, Pease JE, et al. IFN-lambda resolves inflammation via suppression of neutrophil infiltration and IL-1beta production. *J Exp Med*. 2015; 212(6):845–853. <https://doi.org/10.1084/jem.20140995> PMID: 25941255
20. Broggi A, Tan Y, Granucci F, Zanoni I. IFN-lambda suppresses intestinal inflammation by non-translational regulation of neutrophil function. *Nat Immunol*. 2017; 18(10):1084–1093. <https://doi.org/10.1038/ni.3821> PMID: 28846084
21. Koltsida O, Hausding M, Stavropoulos A, Koch S, Tzelepis G, Ubel C, et al. IL-28A (IFN-lambda2) modulates lung DC function to promote Th1 immune skewing and suppress allergic airway disease. *EMBO Mol Med*. 2011; 3(6):348–361. <https://doi.org/10.1002/emmm.201100142> PMID: 21538995

22. Yan B, Chen F, Xu L, Wang Y, Wang X. Interleukin-28B dampens airway inflammation through up-regulation of natural killer cell-derived IFN-gamma. *Sci Rep.* 2017; 7(1):3556. <https://doi.org/10.1038/s41598-017-03856-w> PMID: 28620197
23. Jilg N, Lin W, Hong J, Schaefer EA, Wolski D, Meixong J, et al. Kinetic differences in the induction of interferon stimulated genes by interferon-alpha and interleukin 28B are altered by infection with hepatitis C virus. *Hepatology.* 2014; 59(4):1250–1261. <https://doi.org/10.1002/hep.26653> PMID: 23913866
24. Pervolaraki K, Rastgou Talemi S, Albrecht D, Bormann F, Bamford C, Mendoza JL, et al. Differential induction of interferon stimulated genes between type I and type III interferons is independent of interferon receptor abundance. *PLoS Pathog.* 2018; 14(11):e1007420. <https://doi.org/10.1371/journal.ppat.1007420> PMID: 30485383
25. Galani IE, Triantafyllia V, Eleminiadou EE, Koltsida O, Stavropoulos A, Manioudaki M, et al. Interferon-lambda Mediates Non-redundant Front-Line Antiviral Protection against Influenza Virus Infection without Compromising Host Fitness. *Immunity.* 2017; 46(5):875–890.e876. <https://doi.org/10.1016/j.immuni.2017.04.025> PMID: 28514692
26. Forero A, Ozarkar S, Li H, Lee CH, Hemann EA, Nadsombati MS, et al. Differential Activation of the Transcription Factor IRF1 Underlies the Distinct Immune Responses Elicited by Type I and Type III Interferons. *Immunity.* 2019; 51(3):451–464.e456. <https://doi.org/10.1016/j.immuni.2019.07.007> PMID: 31471108
27. Hamming OJ, Terczynska-Dyla E, Vieyres G, Dijkman R, Jorgensen SE, Akhtar H, et al. Interferon lambda 4 signals via the IFNlambda receptor to regulate antiviral activity against HCV and coronaviruses. *EMBO J.* 2013; 32(23):3055–3065. <https://doi.org/10.1038/emboj.2013.232> PMID: 24169568
28. Doyle SE, Schreckhise H, Khuu-Duong K, Henderson K, Rosler R, Storey H, et al. Interleukin-29 uses a type 1 interferon-like program to promote antiviral responses in human hepatocytes. *Hepatology.* 2006; 44(4):896–906. <https://doi.org/10.1002/hep.21312> PMID: 17006906
29. Dumoutier L, Tounsi A, Michiels T, Sommereyns C, Kotenko SV, Renauld JC. Role of the interleukin (IL)-28 receptor tyrosine residues for antiviral and antiproliferative activity of IL-29/interferon-lambda 1: similarities with type I interferon signaling. *J Biol Chem.* 2004; 279(31):32269–32274. <https://doi.org/10.1074/jbc.M404789200> PMID: 15166220
30. Zhou Z, Hamming OJ, Ank N, Paludan SR, Nielsen AL, Hartmann R. Type III interferon (IFN) induces a type I IFN-like response in a restricted subset of cells through signaling pathways involving both the Jak-STAT pathway and the mitogen-activated protein kinases. *J Virol.* 2007; 81(14):7749–7758. <https://doi.org/10.1128/JVI.02438-06> PMID: 17507495
31. Meager A, Visvalingam K, Dilger P, Bryan D, Wadhwa M. Biological activity of interleukins-28 and -29: comparison with type I interferons. *Cytokine.* 2005; 31(2):109–118. <https://doi.org/10.1016/j.cyto.2005.04.003> PMID: 15899585
32. Sommereyns C, Paul S, Staeheli P, Michiels T. IFN-lambda (IFN-lambda) is expressed in a tissue-dependent fashion and primarily acts on epithelial cells in vivo. *PLoS Pathog.* 2008; 4(3):e1000017. <https://doi.org/10.1371/journal.ppat.1000017> PMID: 18369468
33. Baldrige MT, Lee S, Brown JJ, McAllister N, Urbanek K, Dermody TS, et al. Expression of *Irfn1* on Intestinal Epithelial Cells Is Critical to the Antiviral Effects of Interferon Lambda against Norovirus and Reovirus. *J Virol.* 2017; 91(7):e02079–02016. <https://doi.org/10.1128/JVI.02079-16> PMID: 28077655
34. Corry J, Arora N, Good CA, Sadovsky Y, Coyne CB. Organotypic models of type III interferon-mediated protection from Zika virus infections at the maternal-fetal interface. *Proc Natl Acad Sci U S A.* 2017; 114(35):9433–9438. <https://doi.org/10.1073/pnas.1707513114> PMID: 28784796
35. Witte K, Gruetz G, Volk HD, Looman AC, Asadullah K, Sterry W, et al. Despite IFN-lambda receptor expression, blood immune cells, but not keratinocytes or melanocytes, have an impaired response to type III interferons: implications for therapeutic applications of these cytokines. *Genes Immun.* 2009; 10(8):702–714. <https://doi.org/10.1038/gene.2009.72> PMID: 19798076
36. Dai J, Megjugorac NJ, Gallagher GE, Yu RY, Gallagher G. IFN-lambda1 (IL-29) inhibits GATA3 expression and suppresses Th2 responses in human naive and memory T cells. *Blood.* 2009; 113(23):5829–5838. <https://doi.org/10.1182/blood-2008-09-179507> PMID: 19346497
37. de Groen RA, Boltjes A, Hou J, Liu BS, McPhee F, Friborg J, et al. IFN-lambda-mediated IL-12 production in macrophages induces IFN-gamma production in human NK cells. *Eur J Immunol.* 2015; 45(1):250–259. <https://doi.org/10.1002/eji.201444903> PMID: 25316442
38. Depla M, Pelletier S, Bedard N, Brunaud C, Bruneau J, Shoukry NH. IFN-lambda3 polymorphism indirectly influences NK cell phenotype and function during acute HCV infection. *Immun Inflamm Dis.* 2016; 4(3):376–388. <https://doi.org/10.1002/iid3.122> PMID: 27621819

39. Dickensheets H, Sheikh F, Park O, Gao B, Donnelly RP. Interferon-lambda (IFN-lambda) induces signal transduction and gene expression in human hepatocytes, but not in lymphocytes or monocytes. *J Leukoc Biol.* 2013; 93(3):377–385. <https://doi.org/10.1189/jlb.0812395> PMID: 23258595
40. Liu MQ, Zhou DJ, Wang X, Zhou W, Ye L, Li JL, et al. IFN-lambda3 inhibits HIV infection of macrophages through the JAK-STAT pathway. *PLoS One.* 2012; 7(4):e35902. <https://doi.org/10.1371/journal.pone.0035902> PMID: 22558263
41. Megjugorac NJ, Gallagher GE, Gallagher G. Modulation of human plasmacytoid DC function by IFN-lambda1 (IL-29). *J Leukoc Biol.* 2009; 86(6):1359–1363. <https://doi.org/10.1189/jlb.0509347> PMID: 19759281
42. O'Connor KS, Ahlenstiel G, Suppiah V, Schibeci S, Ong A, Leung R, et al. IFNL3 mediates interaction between innate immune cells: Implications for hepatitis C virus pathogenesis. *Innate Immun.* 2014; 20(6):598–605. <https://doi.org/10.1177/1753425913503385> PMID: 24045339
43. Yin Z, Dai J, Deng J, Sheikh F, Natalia M, Shih T, et al. Type III IFNs are produced by and stimulate human plasmacytoid dendritic cells. *J Immunol.* 2012; 189(6):2735–2745. <https://doi.org/10.4049/jimmunol.1102038> PMID: 22891284
44. Kelly A, Robinson MW, Roche G, Biron CA, O'Farrelly C, Ryan EJ. Immune Cell Profiling of IFN-lambda Response Shows pDCs Express Highest Level of IFN-lambdaR1 and Are Directly Responsive Via the JAK-STAT Pathway. *J Interferon Cytokine Res.* 2016; 36(12):671–680. <https://doi.org/10.1089/jir.2015.0169> PMID: 27617757
45. de Groen RA, Groothuisink ZM, Liu BS, Boonstra A. IFN-lambda is able to augment TLR-mediated activation and subsequent function of primary human B cells. *J Leukoc Biol.* 2015; 98(4):623–630. <https://doi.org/10.1189/jlb.3A0215-041RR> PMID: 26130701
46. Espinosa V, Dutta O, McElrath C, Du P, Chang YJ, Cicciarelli B, et al. Type III interferon is a critical regulator of innate antifungal immunity. *Sci Immunol.* 2017; 2(16).
47. Egli A, Santer DM, O'Shea D, Barakat K, Syedbasha M, Vollmer M, et al. IL-28B is a key regulator of B- and T-cell vaccine responses against influenza. *PLoS Pathog.* 2014; 10(12):e1004556. <https://doi.org/10.1371/journal.ppat.1004556> PMID: 25503988
48. Santer DM, Minty GES, Mohamed A, Baldwin L, Bhat R, Joyce M, et al. A novel method for detection of IFN-lambda 3 binding to cells for quantifying IFN-lambda receptor expression. *J Immunol Methods.* 2017; 445:15–22. <https://doi.org/10.1016/j.jim.2017.03.001> PMID: 28274837
49. Jarret A, McFarland AP, Horner SM, Kell A, Schwerk J, Hong M, et al. Hepatitis-C-virus-induced microRNAs dampen interferon-mediated antiviral signaling. *Nat Med.* 2016; 22(12):1475–1481. <https://doi.org/10.1038/nm.4211> PMID: 27841874
50. Jordan WJ, Eskdale J, Boniotto M, Rodia M, Kellner D, Gallagher G. Modulation of the human cytokine response by interferon lambda-1 (IFN-lambda1/IL-29). *Genes Immun.* 2007; 8(1):13–20. <https://doi.org/10.1038/sj.gene.6364348> PMID: 17082759
51. Gray RD, Hardisty G, Regan KH, Smith M, Robb CT, Duffin R, et al. Delayed neutrophil apoptosis enhances NET formation in cystic fibrosis. *Thorax.* 2018; 73(2):134–144. <https://doi.org/10.1136/thoraxjnl-2017-210134> PMID: 28916704
52. Kajjume T, Kobayashi M. Human granulocytes undergo cell death via autophagy. *Cell Death Discov.* 2018; 4:111. <https://doi.org/10.1038/s41420-018-0131-9> PMID: 30534419
53. Xu Y, Loison F, Luo HR. Neutrophil spontaneous death is mediated by down-regulation of autocrine signaling through GPCR, PI3Kgamma, ROS, and actin. *Proc Natl Acad Sci U S A.* 2010; 107(7):2950–2955. <https://doi.org/10.1073/pnas.0912717107> PMID: 20133633
54. Su AI, Wiltshire T, Batalov S, Lapp H, Ching KA, Block D, et al. A gene atlas of the mouse and human protein-encoding transcriptomes. *Proc Natl Acad Sci U S A.* 2004; 101(16):6062–6067. <https://doi.org/10.1073/pnas.0400782101> PMID: 15075390
55. Uhlen M, Karlsson MJ, Zhong W, Tebani A, Pou C, Mikes J, et al. A genome-wide transcriptomic analysis of protein-coding genes in human blood cells. *Science.* 2019; 366(6472).
56. Levine SJ. Mechanisms of soluble cytokine receptor generation. *J Immunol.* 2004; 173(9):5343–5348. <https://doi.org/10.4049/jimmunol.173.9.5343> PMID: 15494479
57. Jordan WJ, Eskdale J, Srinivas S, Pekarek V, Kellner D, Rodia M, et al. Human interferon lambda-1 (IFN-lambda1/IL-29) modulates the Th1/Th2 response. *Genes Immun.* 2007; 8(3):254–261. <https://doi.org/10.1038/sj.gene.6364382> PMID: 17361203
58. Caron G, Duluc D, Fremaux I, Jeannin P, David C, Gascan H, et al. Direct stimulation of human T cells via TLR5 and TLR7/8: flagellin and R-848 up-regulate proliferation and IFN-gamma production by memory CD4+ T cells. *J Immunol.* 2005; 175(3):1551–1557. <https://doi.org/10.4049/jimmunol.175.3.1551> PMID: 16034093

59. Stevenson M, Stanwick TL, Dempsey MP, Lamonica CA. HIV-1 replication is controlled at the level of T cell activation and proviral integration. *EMBO J.* 1990; 9(5):1551–1560. PMID: [2184033](#)
60. Zack JA, Arrigo SJ, Weitsman SR, Go AS, Haislip A, Chen IS. HIV-1 entry into quiescent primary lymphocytes: molecular analysis reveals a labile, latent viral structure. *Cell.* 1990; 61(2):213–222. [https://doi.org/10.1016/0092-8674\(90\)90802-I](https://doi.org/10.1016/0092-8674(90)90802-I) PMID: [2331748](#)
61. Liu BS, Janssen HL, Boonstra A. IL-29 and IFNalpha differ in their ability to modulate IL-12 production by TLR-activated human macrophages and exhibit differential regulation of the IFNgamma receptor expression. *Blood.* 2011; 117(8):2385–2395. <https://doi.org/10.1182/blood-2010-07-298976> PMID: [21190998](#)
62. Kotenko SV, Izotova LS, Mirochnitchenko OV, Esterova E, Dickensheets H, Donnelly RP, et al. Identification, cloning, and characterization of a novel soluble receptor that binds IL-22 and neutralizes its activity. *J Immunol.* 2001; 166(12):7096–7103. <https://doi.org/10.4049/jimmunol.166.12.7096> PMID: [11390454](#)
63. Xu W, Presnell SR, Parrish-Novak J, Kindsvogel W, Jaspers S, Chen Z, et al. A soluble class II cytokine receptor, IL-22RA2, is a naturally occurring IL-22 antagonist. *Proc Natl Acad Sci U S A.* 2001; 98(17):9511–9516. <https://doi.org/10.1073/pnas.171303198> PMID: [11481447](#)
64. Samarajiwa SA, Mangan NE, Hardy MP, Najdovska M, Dubach D, Braniff SJ, et al. Soluble IFN receptor potentiates in vivo type I IFN signaling and exacerbates TLR4-mediated septic shock. *J Immunol.* 2014; 192(9):4425–4435. <https://doi.org/10.4049/jimmunol.1302388> PMID: [24696235](#)
65. Davidson S, McCabe TM, Crotta S, Gad HH, Hessel EM, Beinke S, et al. IFNlambda is a potent anti-influenza therapeutic without the inflammatory side effects of IFNalpha treatment. *EMBO Mol Med.* 2016; 8(9):1099–1112. <https://doi.org/10.15252/emmm.201606413> PMID: [27520969](#)
66. Muir AJ, Arora S, Everson G, Flisiak R, George J, Ghalib R, et al. A randomized phase 2b study of peginterferon lambda-1a for the treatment of chronic HCV infection. *J Hepatol.* 2014; 61(6):1238–1246. <https://doi.org/10.1016/j.jhep.2014.07.022> PMID: [25064437](#)
67. Phillips S, Mistry S, Riva A, Cooksley H, Hadzhiolova-Lebeau T, Plavova S, et al. Peg-Interferon Lambda Treatment Induces Robust Innate and Adaptive Immunity in Chronic Hepatitis B Patients. *Front Immunol.* 2017; 8:621. <https://doi.org/10.3389/fimmu.2017.00621> PMID: [28611778](#)
68. Mendoza JL, Schneider WM, Hoffmann HH, Vercauteren K, Jude KM, Xiong A, et al. The IFN-lambda-IFN-lambdaR1-IL-10Rbeta Complex Reveals Structural Features Underlying Type III IFN Functional Plasticity. *Immunity.* 2017; 46(3):379–392. <https://doi.org/10.1016/j.immuni.2017.02.017> PMID: [28329704](#)
69. Misumi I, Whitmire JK. IFN-lambda exerts opposing effects on T cell responses depending on the chronicity of the virus infection. *J Immunol.* 2014; 192(8):3596–3606. <https://doi.org/10.4049/jimmunol.1301705> PMID: [24646741](#)
70. Hemann EA, Green R, Turnbull JB, Langlois RA, Savan R, Gale M Jr. Interferon-lambda modulates dendritic cells to facilitate T cell immunity during infection with influenza A virus. *Nat Immunol.* 2019; 20(8):1035–1045. <https://doi.org/10.1038/s41590-019-0408-z> PMID: [31235953](#)
71. Ye L, Schnepf D, Becker J, Ebert K, Tanriver Y, Bernasconi V, et al. Interferon-lambda enhances adaptive mucosal immunity by boosting release of thymic stromal lymphopoietin. *Nat Immunol.* 2019; 20(5):593–601. <https://doi.org/10.1038/s41590-019-0345-x> PMID: [30886417](#)
72. Serra C, Biolchini A, Mei A, Kotenko S, Dolei A. Type III and I interferons increase HIV uptake and replication in human cells that overexpress CD4, CCR5, and CXCR4. *AIDS Res Hum Retroviruses.* 2008; 24(2):173–180. <https://doi.org/10.1089/aid.2007.0198> PMID: [18240961](#)
73. Tian RR, Guo HX, Wei JF, Yang CK, He SH, Wang JH. IFN-lambda inhibits HIV-1 integration and post-transcriptional events in vitro, but there is only limited in vivo repression of viral production. *Antiviral Res.* 2012; 95(1):57–65. <https://doi.org/10.1016/j.antiviral.2012.04.011> PMID: [22584351](#)
74. Syedbasha M, Linnik J, Santer D, O'Shea D, Barakat K, Joyce M, et al. An ELISA Based Binding and Competition Method to Rapidly Determine Ligand-receptor Interactions. *J Vis Exp.* 2016(109).
75. Goel RR, Wang X, O'Neil LJ, Nakabo S, Hasneen K, Gupta S, et al. Interferon lambda promotes immune dysregulation and tissue inflammation in TLR7-induced lupus. *Proc Natl Acad Sci U S A.* 2020; 117(10):5409–5419. <https://doi.org/10.1073/pnas.1916897117> PMID: [32094169](#)
76. Churchill L, Chilton FH, Resau JH, Bascom R, Hubbard WC, Proud D. Cyclooxygenase metabolism of endogenous arachidonic acid by cultured human tracheal epithelial cells. *Am Rev Respir Dis.* 1989; 140(2):449–459. <https://doi.org/10.1164/ajrccm/140.2.449> PMID: [2504090](#)
77. Maciejewski BA, Jamieson KC, Arnason JW, Kooi C, Wiehler S, Traves SL, et al. Rhinovirus-bacteria coexposure synergistically induces CCL20 production from human bronchial epithelial cells. *Am J Physiol Lung Cell Mol Physiol.* 2017; 312(5):L731–L740. <https://doi.org/10.1152/ajplung.00362.2016> PMID: [28283475](#)
78. Thomas HB, Moots RJ, Edwards SW, Wright HL. Whose Gene Is It Anyway? The Effect of Preparation Purity on Neutrophil Transcriptome Studies. *PLoS One.* 2015; 10(9):e0138982. <https://doi.org/10.1371/journal.pone.0138982> PMID: [26401909](#)

79. Drevets DA, Canono BP, Campbell PA. Measurement of bacterial ingestion and killing by macrophages. *Curr Protoc Immunol*. 2015; 109:14.16.11–17.
80. Vandesompele J, De Preter K, Pattyn F, Poppe B, Van Roy N, De Paepe A, et al. Accurate normalization of real-time quantitative RT-PCR data by geometric averaging of multiple internal control genes. *Genome Biol*. 2002; 3(7):RESEARCH0034.
81. Elahi S, Niki T, Hirashima M, Horton H. Galectin-9 binding to Tim-3 renders activated human CD4+ T cells less susceptible to HIV-1 infection. *Blood*. 2012; 119(18):4192–4204. <https://doi.org/10.1182/blood-2011-11-389585> PMID: 22438246